

24875490



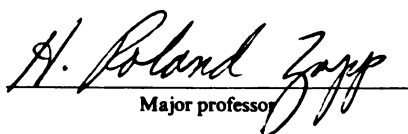
This is to certify that the
dissertation entitled
MEASUREMENT OF APPLE FIRMNESS USING
THE ACOUSTIC IMPULSE RESPONSE

presented by

PAUL ROBERT ARMSTRONG

has been accepted towards fulfillment
of the requirements for

Ph. D. degree in AGRICULTURAL ENGINEERING


Major professor

Date 3/30/89

PLACE IN RETURN BOX to remove this checkout from your record.
TO AVOID FINES return on or before date due.

DATE DUE	DATE DUE	DATE DUE
SEP 22 1988		
SEP 22 1988		
SEP 22 1988		

MSU is An Affirmative Action/Equal Opportunity Institution

MEASUREMENT OF APPLE FIRMNESS USING THE
ACOUSTIC IMPULSE RESPONSE

By

Paul Robert Armstrong

A THESIS

Submitted to
Michigan State University
in partial fulfillment of the requirements
for the degree of

DOCTOR OF PHILOSOPHY

in Agricultural Engineering
Department of Agricultural Engineering

1989

ABSTRACT**MEASUREMENT OF APPLE FIRMNESS USING THE
ACOUSTIC IMPULSE RESPONSE**

By

Paul Robert Armstrong

Non-destructive techniques that could determine fruit maturity or texture would help the producer, packer and retailer achieve a significant improvement in fruit quality. This research investigated the acoustic impulse response of an apple as a non-destructive means of predicting tissue firmness. Resonant frequency modes of an apple were induced by an impulse with the resulting acoustic response being sensed by microphone. Frequency content of the response was elucidated using a Fast Fourier Transform (FFT). The reproducible frequency peak in the spectrum was identified as a resonant mode of the apple. A spherical resonator model, using this resonant frequency, the apple mass and the apple density, was developed to predict the modulus of elasticity. The predicted modulus of elasticity was compared with the measured firmness determined by:

- (1) Magness-Taylor firmness measurements of the apple,
- (2) Classic measurements on apple flesh from which modulus of elasticity was determined.
- (3) Classic measurements on apple tissue which included the

core and flesh in the tissue specimen.

Tests on the apples were conducted over several weeks to investigate the drop in flesh firmness. Regressing the model prediction data on the measured values of firmness show that the model has very good correlation. The r^2 values (correlations) were in the range 0.774-0.803, when the modulus of elasticity measurements included the core of the apple. The model did not have as strong correlations for the Magness-Taylor firmness or for the modulus of elasticity determined only from the apple flesh.

The knowledge gained from this research suggests that the impulse response is satisfactory for non-destructive measurement of the modulus of elasticity of the apple core and surrounding flesh. The ability to predict Magness-Taylor firmness or flesh modulus of elasticity would find greater acceptance by the apple industry. Further research is required to develop the relationship between apple maturity and core strength.

Approved:

H. Roland Zapp
Co-Major Professor

Approved:

John R. Gurnee
Co-Major Professor

Approved:

Donald R. Edwards
Department Chairman

ACKNOWLEDGMENTS

The author would like to express his appreciation to the following people for the encouragement and assistance they gave throughout the course of my graduate program.

To Dr H. Roland Zapp, my major advisor, for his time and effort helping me academically and the hours spent editing this thesis and to Dr. John B. Gerrish, my other advisor, for his enthusiastic support and guidance.

To Dr. Bernie Tennes for helping to initiate and provide assistance for this research.

To Dr. Gary Burgess and Dr. James Resh for their interest and support of this research while serving on my guidance committee.

To Dr. Galen K. Brown for continued interest and support.

To Ed Timm for never failing to answer my questions concerning Wordstar, Plotit etc. and Dick Wolthus for providing technical support.

And to my wife, Tricia, and daughters, Gillian and Claire.

TABLE OF CONTENTS

	PAGE
ACKNOWLEDGMENTS	ii
LIST OF TABLES.	v
LIST OF FIGURES	vi
LIST OF SYMBOLS	vii
 CHAPTER	
1. INTRODUCTION.	1
1.1 The Need	1
1.2 Background.	1
1.3 Objectives	7
2. THEORY OF SPHERICAL RESONATORS.	9
2.1 Strain and Displacement.	9
2.2 Linear Momentum and the Stress Tensor.	10
2.3 Stress-Strain Relationships.	11
2.4 Statement of Dynamic Elasticity.	12
2.5 The Scalar and Vector Potential Problem for a Sphere	15
2.6 Resonant Modes of a Sphere	15
2.6.1 Pure Compressional Modes.	15
2.6.2 Pure Shear Modes.	20
2.6.3 Mixed Modes	21
2.7 Model Development.	21
3. EXPERIMENTAL TECHNIQUES AND PROCEDURES.	24
3.1 Techniques	24
3.1.1 Acoustic Impulse Response Measurement	24
3.1.2 Modulus of Elasticity Measurement	26
3.1.3 Magness-Taylor Measurement.	29
3.1.4 Apple Mass Measurement.	31
3.1.5 Apple Storage	31
3.2 Procedures	31
3.2.1 Controlled Atmosphere (CA) Rome Beauty	32

3.2.2	Controlled Atmosphere (CA)	
	Law Rome.	33
3.2.3	Paula Red	35
3.2.4	Golden Delicious.	37
4.	RESULTS	38
4.1	Magness-Taylor Firmness and Model Predictions.	38
4.2	Elastic Modulus of Flesh and Model Predictions.	40
4.3	Core-Flesh Elastic Moduli and Model Predictions.	42
4.4	Summary of Regression Results.	52
5.	CONCLUSIONS	60
6.	RECOMMENDATIONS FOR FUTURE RESEARCH	62
7.	SUPPLEMENTARY EXPERIMENTATION	64
7.1	Water as the Acoustic Energy Carrier . . .	64
7.2	Signal Noise	65
7.3	Repeatability of the Acoustic Response . .	67
7.4	Experimentation with an Elastic Sphere . .	71
7.5	Signals from an Accelerometer.	72
	APPENDIX	78
	BIBLIOGRAPHY	87

LIST OF TABLES

TABLE	PAGE
4.1 Regression results from the study.	56
7.1 Peak frequency reproducibility of five apples. . .	69
7.2 Peak frequencies obtained from different impulse and receiver orientations for five apples	71
7.3 Comparison of peak frequencies for two apple shapes of the same mass and the spheres from which they were made	73
7.4 Ratios of peak frequencies to center frequency . .	76

LIST OF FIGURES

FIGURE	PAGE
2.1 Spherical coordinate system for the spherical resonator.	16
2.2 Mode chart for the spherical resonator	19
2.3 Particle displacement for lower-order modes.	22
3.1 Instrumentation and apple orientation used to measure the acoustic impulse response.	25
3.2 The digitized acoustic impulse response of an apple detected by the microphone and the frequency spectrum obtained with a FFT	27
3.3 Instrumentation used to measure modulus of elasticity of an apple specimen.	28
3.4 Force versus time curve obtained for modulus of elasticity measurement	30
3.5 Relative location with respect to the apple where specimens were obtained for modulus of elasticity measurement	34
3.6 Apparatus used to obtain the specimens	34
4.1 Predicted modulus of elasticity versus measured Magness-Taylor firmness for CA Rome Beauty apples	39
4.2 Predicted versus measured modulus of elasticity for CA Law Rome apples	41
4.3 Drop in peak frequency versus time of 16 CA Law Rome Apples.	43
4.4 Predicted versus measured modulus of elasticity for Paula Red apples	45
4.5 Predicted versus measured modulus of elasticity for Paula Red apples	46

4.6	Predicted versus measured modulus of elasticity for Paula Red apples	48
4.7	Frequency squared versus measured modulus of elasticity for Paula Red apples.	49
4.8	Predicted versus measured modulus of elasticity for Golden Delicious apples.	50
4.9	Predicted versus measured modulus of elasticity for Golden Delicious apples.	51
4.10	Predicted versus measured modulus of elasticity for Golden Delicious apples.	53
4.11	Frequency squared versus measured modulus of elasticity for Golden Delicious apples	54
4.12	Drop in peak frequency versus time of 10 Golden Delicious Apples	55
7.1	Original acoustic signal and its spectrum.	66
7.2	DC attenuation of the acoustic signal and its spectrum	66
7.3	Two signals and their spectra displaying multiple resonant peaks.	68
7.4	Orientation of impulse and microphone.	70
7.5	Spectra from two apples and the orientation of the receiving device.	75

LIST OF SYMBOLS

A	= area
a	= sphere radius
E	= modulus of elasticity
G	= shear modulus of elasticity
Ω	= normalized frequency
c_l	= longitudinal phase velocity
c_t	= shear phase velocity
c_{ijkl}	= stiffness coefficients
F	= body force
f	= frequency, cycles/s
i	= denotes complex number
J_n	= Bessel functions of the first kind
n_k	= component of a unit vector
m, n	= subscripts
P_n	= Legendres polynomials
u	= displacement
S	= surface
T	= surface traction
t	= time
V	= volume
x, y, z	= cartesian coordinate axes
Z_n	= radial Bessel function
r, θ, ϕ	= spherical coordinate axes

ε	= strain tensor
τ	= stress tensor
δ	= Kronecker delta
ϕ	= scalar potential
ψ	= vector potential
ρ	= density
∇^2	= Laplacian operator
∇	= gradient operator
λ, μ	= Lamé's constants
ν	= Poisson's ratio
ω	= frequency, radians/s
MPa	= pressure units (N/m ²)

I Introduction

1.1 The Need

Texture is an important factor in determining apple maturity and quality. Apart from appearance, apples with good texture are highly desired by consumers. To the grower or fruit handler, it is important that the textural quality of the product be high at the time of delivery to the retailer to maximize profitability. Techniques that could non-destructively measure the texture of individual apples would greatly enhance management decisions during picking, grading and storage operations. These techniques may also be used to great advantage in the study of growth and quality retention in storage. Flesh firmness is used as an indicator of apple texture, maturity and apple flesh strength. Very firm apples are generally desired by the consumer as these are regarded as being fresh and crisp. Techniques suggested by USDA (1978) to determine firmness include Magness-Taylor firmness testing, thumb pressure, wax development, cutting and chewing tests. Often these tests are used in combination. Magness-Taylor firmness testing is the least subjective method used, but Lott (1965) found that it did not consistently correlate with the degree of apple maturity. Since it is a destructive test, it is feasible only as a method to be applied to obtain average firmness

values.

1.2 Background

The general interest in being able to objectively evaluate fruit texture has led to various techniques for characterizing physical properties of fruit tissue in well-defined engineering terms. Conventional modulus of elasticity measurements, as described by Mosehnin (1980), subject regular shaped test specimens of tissue to compressive loadings at constant strain rates. The resulting stress-versus-strain relationship can be used to determine the strength of the tissue in terms of modulus of elasticity. A high modulus of elasticity indicates high tissue strength, which is generally associated with good textural quality in apples.

Because of the spheroidal shape of most agricultural products, the Hertz problem of contact stresses has been considered as a means of determining material properties. Most prominent of the Hertz formulations are the contact of a sphere with another sphere and a sphere with a flat plate. Boussinesq obtained similar type solutions for the contact of a loading die with a semi-infinite medium. Shpolyanskaya (1952) utilized the Hertz formulation in defining the modulus of elasticity of a wheat grain. Fridley (1974) attempted to determine the modulus of elasticity of pears from quasi-static deformation measurements with a steel ball.

Less direct methods for firmness detection consider fruit coloration as a means of determining maturity or

firmness. Bittner and Norris (1968) used light reflectance properties of peaches to discern degree of maturity. The ratio of the reflectance of light at 580 nm to 620 nm wavelengths was found to decrease linearly with respect to picking date. Regressing this ratio onto picking time resulted in correlation coefficients ranging from 0.798 to 0.924 for three different varieties. Correlation was found to be highest using the blushed side of the fruit. Clark and Shackelford (1973) used the same light reflectance ratio to correlate coloration with firmness. Correlation coefficients ranged from 0.43 to 0.72 for different varieties except for the Loring variety which was 0.16. Hood et al. (1976) used a modified FMC color sorter to measure peach surface reflectance at 675 nm. The reflectance value was scaled by a reflectance measurement in the infrared region, 800-1200 nm, which was assumed to be proportional to peach size and was termed the "maturity index". Correlation was significant between this index and measured firmness for the two varieties tested. Delwiche et al. (1981) used the FMC machine interfaced with a computer for data acquisition of maturity index. Firmness correlated well with maturity index except for clingstone varieties.

Impact forces caused by fruit striking a surface have been studied as a means of determining flesh strength. Using a Kelvin model to describe the impact behavior of a tomato, Nahir (1986) was able to utilize characteristics of the impact curve to sort fruits by color with little error.

De Beaerdemaeker et al. (1982) investigated the transformation of fruit impact forces to the frequency domain as a possible means of rapid texture evaluation. Simulated impacts performed by Delwiche et al. (1986) indicated hard fruit had higher impact levels and smaller contact times with flat plates than did soft fruit for equivalent contact velocities. Transformation of the impact curve from the time domain to the frequency domain should yield higher frequency content for harder fruit. Electronic hardware developed by Delwiche et al. (1985) used analog bandpass filters to extract specific components of the frequency spectrum of an impact for analysis and subsequent firmness evaluation.

Resonant frequencies of whole fruit and fruit sections have been used to define flesh strength. Resonant frequency measurements can be achieved in a non-destructive manner with different techniques, thus its potential for use in firmness measurement seems good. Clark and Mikelson (1942) were among the first people to recognize the possibility of non-destructive texture evaluation using vibrational characteristics of fruit. The forced vibrational methods used by Abbott (1968 a,b) were effective in measuring the resonant frequencies of whole apples and apple sections. Flesh firmness was defined in terms of a "stiffness coefficient" for whole apples or modulus of elasticity for apple sections. Abbott (1968 a) used periodic electro-magnetic coupling to drive cylindrical apple sections. Excitation was swept

through a range of frequencies to obtain maximum displacement modes which directly corresponded to resonant frequencies. The specimen was subject to precise boundary conditions from which the modulus of elasticity could be determined using relatively simple mathematics. Whole apples were treated in a similar manner to obtain resonant frequencies with a mechanical driving mechanism attached directly to the apple. Skin vibration was detected by a piezoelectric transducer attached to the apple skin. For whole apples a "stiffness coefficient", $f^2 \cdot m$, was used to relate the apple's vibrational characteristics to flesh firmness. The variable f was considered to be a resonant frequency of the apple and m was the apple mass. The stiffness coefficient was found to decrease with age of the apple. Finney (1971), using similar techniques as Abbott (1968 a) on whole apples, found that sensory evaluations of apples and corresponding $f^2 \cdot m$ values correlated well, although not as well as the Magness-Taylor pressure readings and sensory evaluations. Excitation and response of the apple were determined by attaching the apple to a vibration table and fixing an accelerometer to the top of the apple. The core of the apple was parallel to the horizontal plane of the table. Table frequencies were swept from 100 to 5000 Hz.

Longitudinal resonant frequencies of cylindrical-shaped banana sections were used by Finney et al (1967) to determine modulus of elasticity. Modulus of elasticity values

obtained in this manner correlated well with sugar and starch content of the bananas. Vibration tests conducted by Finney (1971) indicated that peach firmness can be determined by observing the response of the peach when driven mechanically by a 2000 Hz sinusoidal input.

A mechanical impulse applied to an apple produces audible resonant frequencies. Yamamoto (1980) compared Magness-Taylor readings with apple peak frequency components of the acoustic signal when excited by this method. Correlation coefficients obtained from the regression of f , $f^2 \cdot m$ and $f^2 \cdot m^{2/3} \cdot p^{1/3}$, where p is apple density, with Magness-Taylor readings were on the order of 0.75 for Starking Delicious and 0.65 for Golden Delicious. Abbott (1968 b) and Finney (1971) both concluded that resonant frequencies of the apple were dependent on apple mass. There appeared to be little evidence from results by Yamamoto (1980) that support the dependency on mass based on regression results for the different variable combinations that were used.

While the approach of determining apple firmness from natural frequencies is promising, there remain many interacting factors which may account for the variances in natural frequencies obtained from what appear to be similar apples. Among these are apple internal core composition, cellular size and structure. Abbott (1968 a) did determine that the skin strengthens the overall apple. Resonant frequencies of whole apples and peeled apples were compared, revealing that whole apples had higher resonant frequencies.

Cooke (1970) utilized an elastic sphere model to explain some of these factors and to identify the apple frequency modes observed by other researchers. He elaborated on the techniques of excitation and measurement and determined if the modulus of elasticity or if the shear modulus would yield the best correlations for different modes of vibration. Later studies by Cooke (1972, 1973) used a 3-media elastic sphere to represent the structure of an apple and presented an analytical procedure to determine resonant frequencies for this model. The three-layer model consisted of three concentric spheres where the outer layer represented the skin, the middle the flesh and the inner sphere the core. He concluded that the ratio of flesh to skin diameters and densities were generally more important in defining torsional type vibrations whereas core to skin ratios of diameter and densities were important for spheroidal vibrations. Deviation of the true apple shape from a sphere was not modelled.

1.3 Objectives

The objective of this research was to determine if the acoustic impulse response of an apple is a feasible means of determining tissue firmness. While other vibration techniques appear to show promise in determining firmness, the choice to use the impulse technique is based on the relative ease with which it can be implemented both in the laboratory and in a working environment. The approach in realizing the objective was to develop techniques to induce resonant

vibrations in an apple with an impulse, to record and analyze the response that would characterize firmness, and to develop a suitable model to use this information to predict firmness.

II Theory of Spherical Resonators

The development of a model to predict apple tissue firmness was based on the resonant behavior of an elastic sphere. The choice of this model is due largely to the shape similarity with an apple. Resonant behavior in an elastic medium is determined by the medium's modulus of elasticity as well as geometry, density and Poisson's ratio. By suitable manipulation of the fundamental equations which govern resonance of a sphere, a model equation is developed that relates modulus of elasticity to frequency of vibration, mass, density and Poisson's ratio of the elastic medium.

Fundamental relationships governing the dynamic behavior of a medium is presented in the following sections. These relationships, extracted from Auchebach (1973), are applicable to any medium which can be described as possessing homogeneous, isotropic, and linearly elastic physical characteristics.

2.1 Strain and Displacement

Letting the field defining the displacements of particles be denoted by $u(x,t)$. The deformation or strain of a medium can be expressed in terms of the gradient of the displacement vector. Within the restrictions of linearized

theory, the deformation, u , can be described by the small strain tensor, ε , with components

$$\varepsilon_{ij} = \frac{1}{2} (u_{i,j} + u_{j,i}) \quad [1]$$

The subscript i indicates the coordinate direction normal to the elemental area on which the strain acts and the subscript j denotes the the coordinate direction of the strain. The comma denotes differentiation with respect to the subscript following the comma.

2.2 Linear Momentum and the Stress Tensor

Considering a volume V of a medium with S as the boundary: the surface S is subject to surface tractions $T(x,t)$ and each element mass within the volume is subject to body forces per unit mass of $f(x,t)$. A balance of linear momentum of this volume results in:

$$\int_S T \, dA + \int_V \rho f \, dV = \int_V \rho \ddot{u} \, dV \quad [2]$$

Using Cauchy's stress formula,

$$T_i = \tau_{ki} n_k \quad [3]$$

components, τ_{ki} , of the stress tensor, τ , are equated to surface tractions, T_i , where n_k is a component of the unit vector along the outer normal to the surface S . In indicial notation, substitution of equation [3] into [2] results in:

$$\int_s \tau_{kl} n_k dA + \int_v \rho f_l dV - \int_v \rho \ddot{u}_l dV \quad [4]$$

Gauss' theorem can be used to transform the surface integral to a volume integral, so that

$$\int_v (\tau_{kl,k} + \rho f_l - \rho \ddot{u}_l) dV = 0 \quad [5]$$

Wherever the integrand is continuous:

$$\tau_{kl,k} + \rho f_l = \rho \ddot{u}_l \quad [6]$$

2.3 Stress-Strain Relationships

In general terms, the relation between the stress, τ , and strain tensor, ε , is:

$$\tau_{ij} = C_{ijkl} \varepsilon_{kl} \quad [7]$$

The stiffness constants, C_{ijkl} , may be expressed as

$$C_{ijkl} = \lambda \delta_{ij} \delta_{kl} + \mu (\delta_{ik} \delta_{jl} + \delta_{il} \delta_{jk}) \quad [8]$$

where δ is the Kronecker delta and λ and μ are Lamé's constants.

Substitution of [8] into [7] leads to the following form of Hooke's law.

$$\tau_{ij} = \lambda \varepsilon_{kk} \delta_{ij} + 2\mu \varepsilon_{ij} \quad [9]$$

2.4 Statement of Dynamic Elasticity

Consider a body **B** occupying a regular region **V**, which may be bounded or unbounded, with interior **V**, and boundary **S**. The system of equations governing the motion of a homogeneous, isotropic, linearly elastic body consists of the previously developed equations, [1], [6], and [9].

$$\varepsilon_{ij} = \frac{1}{2} (u_{i,j} + u_{j,i}) \quad [10]$$

$$\tau_{ij,j} + \rho f_i = \rho \ddot{u}_i \quad [11]$$

$$\tau_{ij} = \lambda \varepsilon_{kk} \delta_{ij} + 2\mu \varepsilon_{ij} \quad [12]$$

Substituting [10] into [12] and the resulting stress expressions into [11], the following displacement equation of motion is obtained:

$$\mu u_{i,jj} + (\lambda + \mu) u_{j,ji} + \rho f_i = \rho \ddot{u}_i \quad [13]$$

In the absence of body forces equation [13] becomes:

$$\mu u_{i,jj} + (\lambda + \mu) u_{j,ji} = \rho \ddot{u}_i \quad [14]$$

In vector notation this can be represented as:

$$\mu \nabla^2 \mathbf{u} + (\lambda + \mu) \nabla \nabla \cdot \mathbf{u} = \rho \ddot{\mathbf{u}} \quad [15]$$

where ∇^2 and ∇ are the Laplacian and gradient operators, respectively.

A decomposition of the displacement vector to scalar, ϕ , and vector potential, ψ , functions gives:

$$\mathbf{u} = \nabla \phi + \nabla \times \psi \quad [16]$$

Conditions on the displacement representation to satisfy the equation of motion are found by substitution of [16] into [15] yielding:

$$\begin{aligned} \mu \nabla^2 [\nabla \phi + \nabla \times \psi] + (\lambda + \mu) \nabla \nabla \cdot [\nabla \phi + \nabla \times \psi] \\ = \rho \frac{\partial^2}{\partial t^2} [\nabla \phi + \nabla \times \psi] \end{aligned} \quad [17]$$

Rearranging terms and using the relationships $\nabla \cdot \nabla \times \psi = 0$ and $\nabla \cdot \nabla \phi = \nabla^2 \phi$ results in:

$$\nabla [(\lambda + 2\mu) \nabla^2 \phi - \rho \ddot{\phi}] + \nabla \times [\mu \nabla^2 \psi - \rho \ddot{\psi}] = 0 \quad [18]$$

The displacement representation [16] will satisfy the equation of motion if:

$$\nabla^2 \phi = \frac{1}{C_1^2} \ddot{\phi} \quad [19]$$

$$\nabla^2 \psi = \frac{1}{c_t^2} \ddot{\psi} \quad [20]$$

where:

$$c_l = \left[\frac{(\lambda + 2\mu)}{\rho} \right]^{\frac{1}{2}} \quad [21]$$

$$c_t = \left[\frac{\mu}{\rho} \right]^{\frac{1}{2}} \quad [22]$$

c_l and c_t are termed the compressional (longitudinal) and shear (transverse) phase velocities, respectively.

For time harmonic fields with frequency ω , equations [19] and [20] may be written, Auld (1973):

$$\nabla^2 \phi + \frac{\omega^2}{c_l^2} \phi = 0 \quad [23]$$

$$\nabla^2 \psi + \frac{\omega^2}{c_t^2} \psi = 0 \quad [24]$$

Equation [16] relates the three components of the displacement vector to four other functions: the scalar potential and the three components of the vector potential. This indicates that an additional constraint is required. For an unbounded medium subjected to a distribution of body forces, with arbitrary initial conditions, Achenbach (1973) shows the following condition is sufficient to meet this requirement.

$$\nabla \cdot \psi = 0 \quad [25]$$

2.5 The Scalar and Vector Potential Problem for a Sphere

The spherical coordinate representation used in the following development is shown in figure 2.1.

Solutions of the scalar potential equation [23] in spherical coordinates, as given by Stratton (1941), have the general form:

$$\phi_{mn}(r\theta\phi) = Z_n \left(\frac{\omega r}{c_l} \right) P_n^{|m|}(\cos\theta) e^{im\phi} \quad [26]$$

where $n = 0, 1, 2, \dots$ and $-n < m < n$.

The dependence of the function on θ is given by Legendre polynomials of the first kind. Radial Bessel functions describe the radial functional dependence. Similarly for the vector potential:

$$\psi_{mn}(r\theta\phi) = Z_n \left(\frac{\omega r}{c_t} \right) P_n^{|m|}(\cos\theta) e^{im\phi} \quad [27]$$

2.6 Resonant Modes of a Sphere

2.6.1 Pure Compressional Modes

For a solid spherical resonator of radius a , solutions given by [26] and [27] must remain finite at $r=0$ thus only Bessel functions of the first kind, j_n , may be used. When $m=n=0$, solutions for [26] and [16] are:

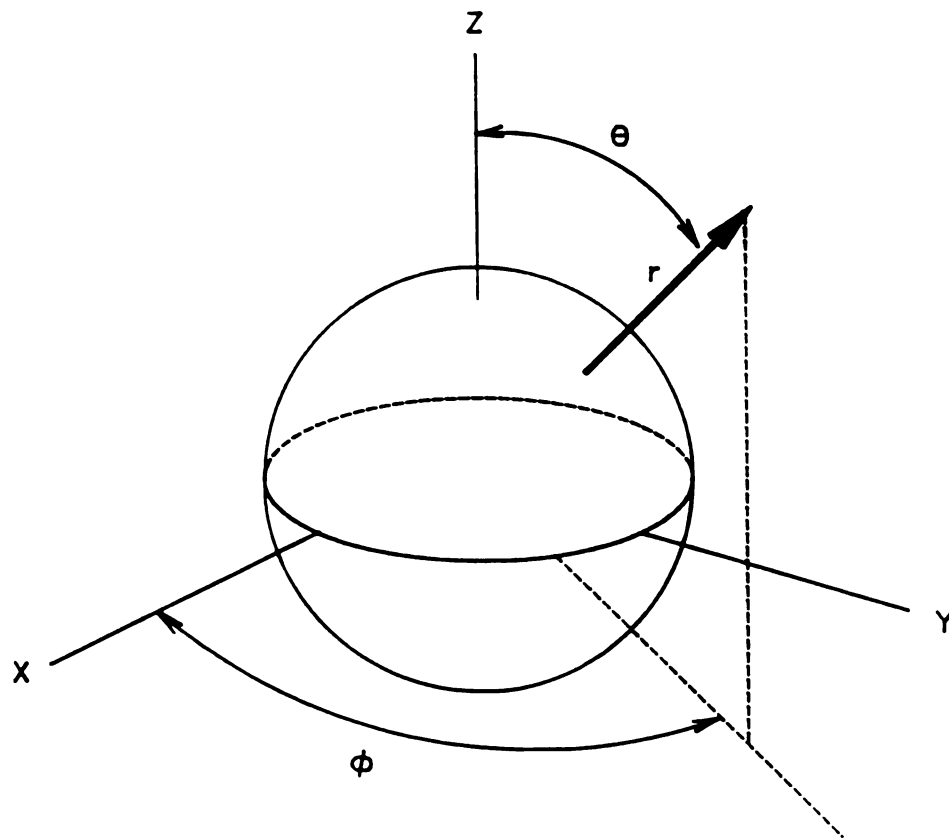


Figure 2.1 Spherical coordinate system for the spherical resonator.

$$u_{mn} = u_{00} - \nabla j_0 \left(\frac{\omega r}{c_l} \right) = \hat{r} \frac{\partial}{\partial r} j_0 \left(\frac{\omega r}{c_l} \right) \quad [28]$$

where \hat{r} is the radial unit vector.

The strain field corresponding to this, from equation [10], has only three components:

$$\varepsilon_{rr} = \frac{1}{i\omega} \frac{\partial u_r}{\partial r} \quad [29 \text{ a.}]$$

$$\varepsilon_{\theta\theta} = \frac{1}{i\omega} \frac{u_r}{r} \quad [29 \text{ b.}]$$

$$\varepsilon_{\phi\phi} = \frac{1}{i\omega} \frac{u_r}{r} \quad [29 \text{ c.}]$$

and the traction force on the spherical surface from equations [3] and [12] is:

$$T \cdot \hat{r} = T_{rr} = C_{11} \varepsilon_{rr} + C_{12} (\varepsilon_{\theta\theta} + \varepsilon_{\phi\phi}) \quad [30]$$

where C_{11} and C_{12} are elements of the stiffness matrix, Auld (1973). For the assumptions governing this medium, Lamé's constants can be equated to the stiffness coefficients by,

$$\lambda = C_{12} \quad \text{and} \quad \mu = C_{44}$$

Equations [28] to [30] lead to a stress free boundary condition of:

$$c_{11} \frac{\partial^2}{\partial r^2} j_0\left(\frac{\omega r}{c_1}\right) + \frac{2c_{12}}{r} \frac{\partial}{\partial r} j_0\left(\frac{\omega r}{c_1}\right) = 0 \quad [31]$$

At $r = a$, the substitution of an approximation for the radial Bessel function for $n=0$ (first kind, zero order)

$$j_0\left(\frac{\omega r}{c_1}\right) = \frac{\sin(\omega r/c_1)}{(\omega r/c_1)}$$

leads to the characteristic frequency equation:

$$\tan\left(\frac{\omega a}{c_1}\right) = \frac{\left(\frac{\omega a}{c_1}\right)}{1 - \frac{c_{11}}{4c_{44}} \left(\frac{\omega a}{c_1}\right)^2} \quad [32]$$

Specific values of ω which satisfy this equation are listed in various references, Auld (1973), Love (1949), Eringen (1974). These modes are designated S_{0l} where l refers to the order of roots which satisfy [32]. Introduction of the normalized frequency, Ω , defined by:

$$\Omega = \frac{\omega a}{c_t}$$

provides a common way of expressing frequencies between modes. Figure 2.2 shows the normalized frequency as a function of Poisson's ratio. c_t can be equated to c_1 by:

$$c_t = c_1 \left(\frac{1-2\nu}{2(1-\nu)} \right)^{\frac{1}{2}} \quad [33]$$

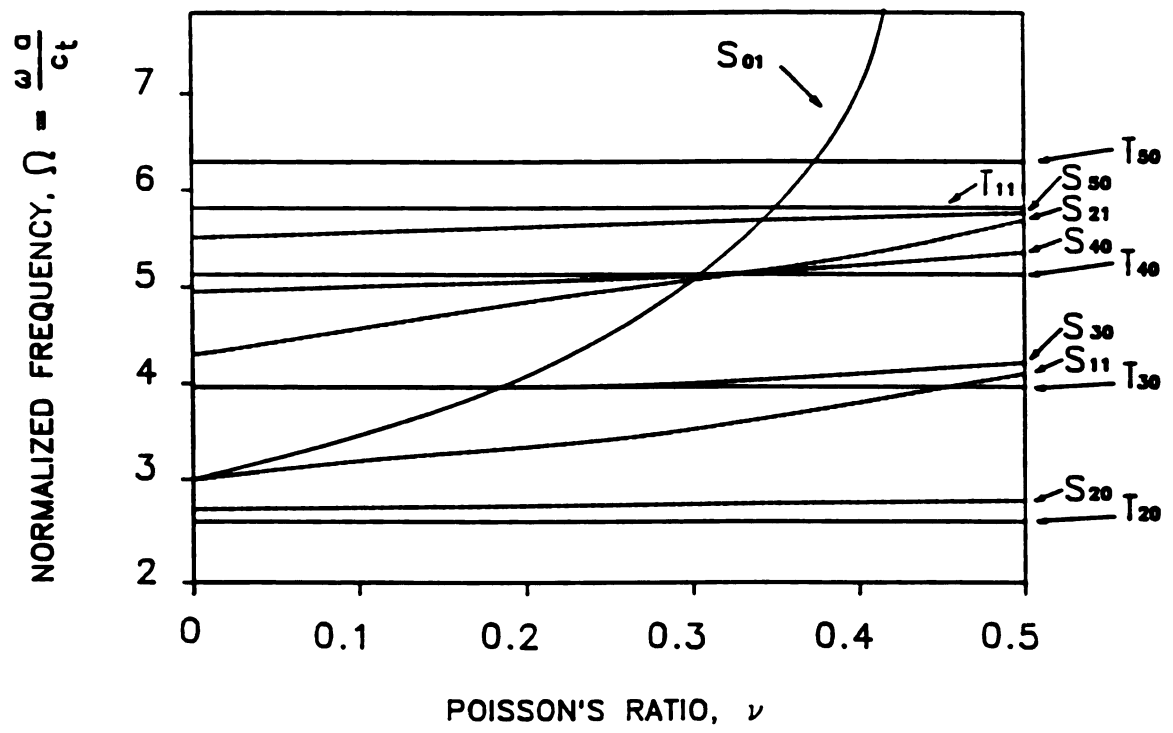


Figure 2.2 Mode chart for the spherical resonator.

2.6.2 Pure Shear Modes

Particle motion for this mode is always normal to the radial coordinate. From equations [16] and [27], particle motion is:

$$u_{\theta} = \frac{1}{\sin \Theta} \frac{\partial \psi_{mn}}{\partial \phi} \quad [34]$$

$$u_{\phi} = \frac{\partial \psi_{mn}}{\partial \Theta} \quad [35]$$

Bessel functions of the first kind are again only valid and the strain field from equation [10] has components which include only:

$$\varepsilon_{\theta\theta}, \varepsilon_{\phi\phi}, \varepsilon_{r\theta}, \varepsilon_{r\phi}, \varepsilon_{\theta\phi}$$

Traction force on the sphere from equation [3] is:

$$\tau \cdot \hat{r} = \hat{\Theta} \frac{c_{44}}{i\omega} \left(\frac{\partial u_{\theta}}{\partial r} - \frac{u_{\theta}}{r} \right) + \hat{\Phi} \frac{c_{44}}{i\omega} \left(\frac{\partial u_{\phi}}{\partial r} - \frac{u_{\phi}}{r} \right) \quad [36]$$

where $\hat{\Theta}$ and $\hat{\Phi}$ are the spherical unit vectors.

For $m=0, n=1$ the particle field velocity from equations [27] and [16] is:

$$u_{\theta 1} = \hat{\Phi} \frac{\partial}{\partial \Theta} \psi_{01} = -\hat{\Phi} \cos \Theta j_1 \left(\frac{\omega r}{c_t} \right) \quad [37]$$

Particle motion is a rigid rotation of spherical shells about the z-axis with adjacent shells moving in opposite directions. The characteristic frequency equation for this case is:

$$\tan \left(\frac{\omega a}{C_1} \right) = \frac{\left(\frac{\omega a}{C_1} \right)}{1 - \frac{C_{11}}{4C_{44}} \left(\frac{\omega a}{C_1} \right)^2} \quad [38]$$

Shear modes are designated $T_{n,1-1}$ where 1 refers to the order of roots which satisfy equation [38]. Figure 2.2 shows the normalized frequency, Ω , as being independent of Poisson's ratio. Frequencies are not dependent on the subscript m thus it is dropped. Note for $n=1$ the second mode subscript is chosen to be 1 rather than 1-1 according to common convention, Auld (1973).

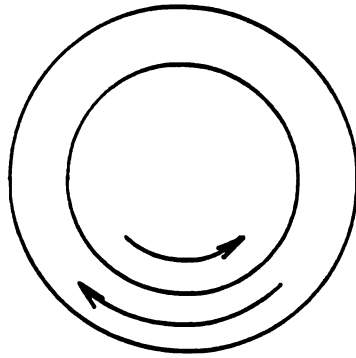
2.6.3 Mixed Modes

Stress-free boundary conditions at $r = a$ result in complicated frequency relations for specific cases. These modes are designated $S_{n,1-1}$ and are shown in figure 2.2 for several lower-order modes. Solutions for specific cases were calculated by Sato et al. (1962). General particle displacement of lower-order modes for the three modes are shown in figure 2.3.

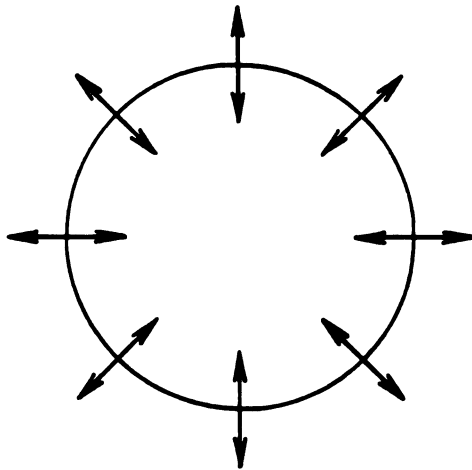
2.7 Model Development

Utilizing equation [22], standard identities for elastic constants and the normalized frequency notation, the shear modulus, G , for a particular vibrational mode can be determined from:

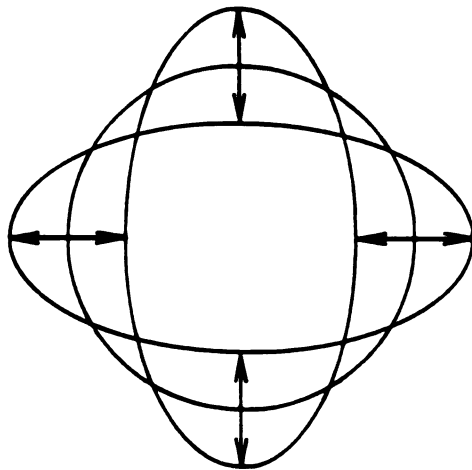
$$G = \left(\frac{\omega a}{\Omega} \right)^2 \rho \quad [39]$$



The lowest-order torsional mode of a spherical resonator designated the T_{11} mode.



The lowest frequency mode of radial compression, S_{01} , called the breathing mode.



The lowest frequency mode of a spherical resonator in a mixed mode, S_{20} , called the oblate-prolate mode.

Figure 2.3 Particle displacement for lower-order modes.

In terms of density, mass and frequency this becomes:

$$G = \left[\frac{\rho^{1/3} (6\pi^2)^{2/3}}{\Omega^2} \right] f^2 m^{2/3} \quad [40]$$

or in terms of the Elastic Modulus, E :

$$E = \left[\frac{\rho^{1/3} (6\pi^2)^{2/3} 2(1+\nu)}{\Omega^2} \right] f^2 m^{2/3} \quad [41]$$

Equation [41] provides a useful model for determining material property strengths of apple tissue utilizing the quantities of mass, density, frequency of vibration, and Poisson's ratio. The mode of vibration is also fundamentally important. This equation will be used to predict modulus of elasticity values of apple tissue for comparison with measured values of tissue firmness.

III EXPERIMENTAL TECHNIQUES AND PROCEDURES

3.1 Techniques

3.1.1 Acoustic Impulse Response Measurement

Yamamoto (1980) utilized the acoustic impulse response technique to measure the resonant frequencies of apples. Although his results did not identify any dependence or independence on the variables he used in a model to predict firmness, he did have good correlations for the models used and provided insight on impulsive techniques for apples.

For this study an apple was struck by a hammer which consisted of a ball of bees wax attached to the end of a steel rod. The ball of the hammer was approximately 2 cm in diameter. Acoustic emissions from the apple were sensed by a Radio Shack electret 270-090 microphone and the signal stored on a Analogic Model 6000 digitizing oscilloscope. A schematic diagram of the instrumentation and apple orientation is illustrated in figure 3.1. The microphone was positioned near the equator of the apple. Apples were held by hand, approximately 1 cm in front of the microphone and struck on the opposite side of the fruit.

The acoustic signal emitted by the apple triggered the oscilloscope, which then sampled the signal at a rate of 25 KHz, or every 40 micro-s, for a total of 2048 points. Data were stored on floppy disk, as digitized voltage levels. A

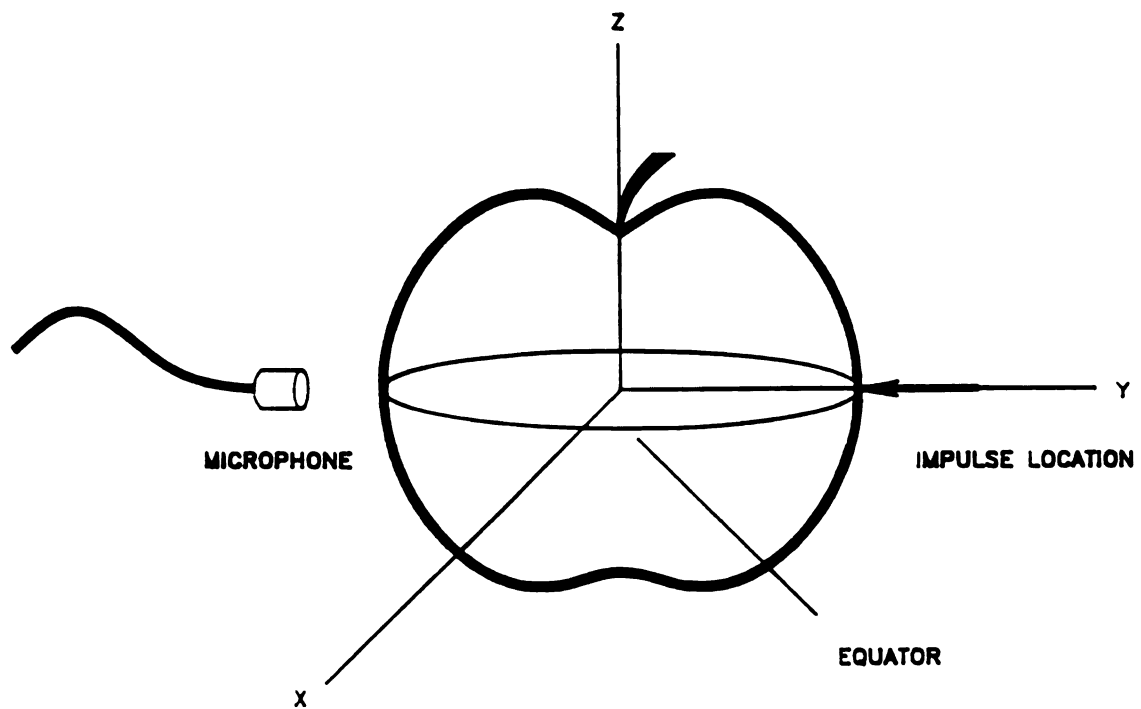
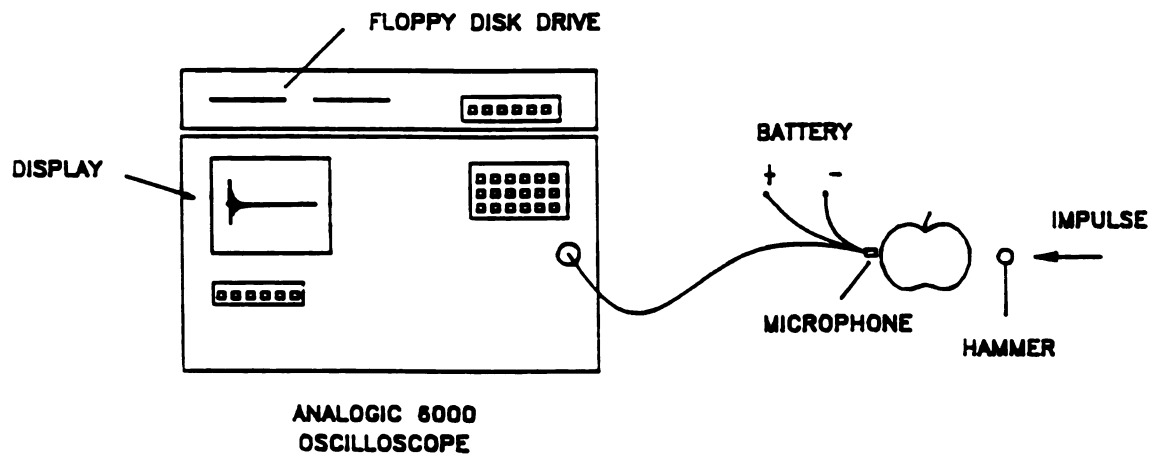


Figure 3.1 Instrumentation and apple orientation used to measure the acoustic impulse response.

Fast Fourier Transform, FFT, of the digital signal was performed by the oscilloscope, and in some cases by a personal computer, to determine frequency content. Figure 3.2 shows a typical sampled acoustic signal from an apple and the frequency spectrum of this signal. Resolution of the FFT is determined by $1/NT$ where N is the number of points sampled and T is the sampling period in seconds. A sampling period of 40 micro-s, for 2048 total points results in the resolution of the FFT to be 12.207 Hz over an effective range of 0-12.5 KHz.

3.1.2 Modulus of Elasticity Measurement

Modulus of Elasticity measurements were obtained by subjecting a test specimen from the apple to a uniform axial compression test as shown in figure 3.3. A Daytronic 152a+50 load cell was fixed to a Chatillon HTCM crosshead. Apple sections were placed between parallel plates, one plate being attached to the load cell the other was the moving base of the Chatillon HTCM. Base plate speed was set at 0.05 cm/s for all testing. Signal output from the load cell was amplified with a Daytronic 300D amplifier before being fed to the Analogic 6000 oscilloscope. Input to the oscilloscope was sampled every 15 ms for a total of 1000 points. Load cell calibration, expressed in volts/kg, was done prior to testing and checked after test completion. Recordings of force versus time, taken by the oscilloscope, were transferred to floppy disk and analyzed on an IBM AT computer utilizing a plotting and signal analysis program

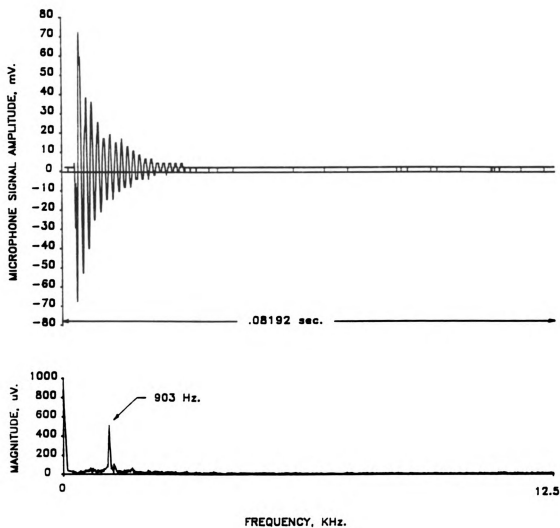


Figure 3.2 The digitized acoustic impulse response of an apple detected by the microphone and the frequency spectrum obtained with a FFT.

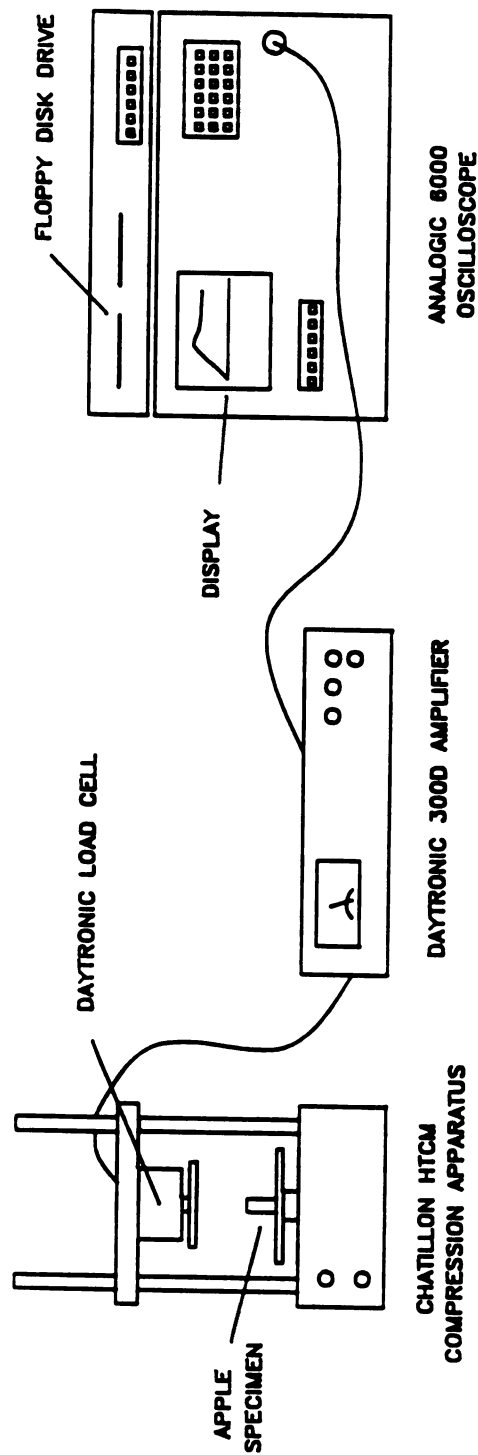


Figure 3.3 Instrumentation used to measure modulus of elasticity of an apple specimen.

developed by the author. Modulus of elasticity was estimated by determining the slope, expressed in N/sec, of the linear section of the plot by linear regression. The slope was used to form a line, passing through zero, which represented force versus compression (expressed in meters) of the specimen. The compression of the specimen was obtained by consideration of the crosshead speed. The transformation of the slope units of N/m to stress/strain, as a result of dividing by the specimen cross-sectional area and original specimen length, yields modulus of elasticity. Figure 3.4 shows a typical plot and the linear section used in calculating the modulus of elasticity. Test specimen size and the location from the apple, varied between experiments as detailed in section 3.2.

3.1.3 Magness Taylor Measurement

Magness Taylor readings were performed with a Chatillon HTCM firmness tester. This was the same instrument used in modulus of elasticity measurements with a firmness testing plunger substituted for the load cell. The 11.1 mm diameter plunger was driven into the apple by a variable speed electric motor to an approximate depth of 15 mm. Speed was set at approximately 10 cm/min for all tests. Skin and some flesh was removed from the apple to provide a relatively flat surface of contact for the plunger.

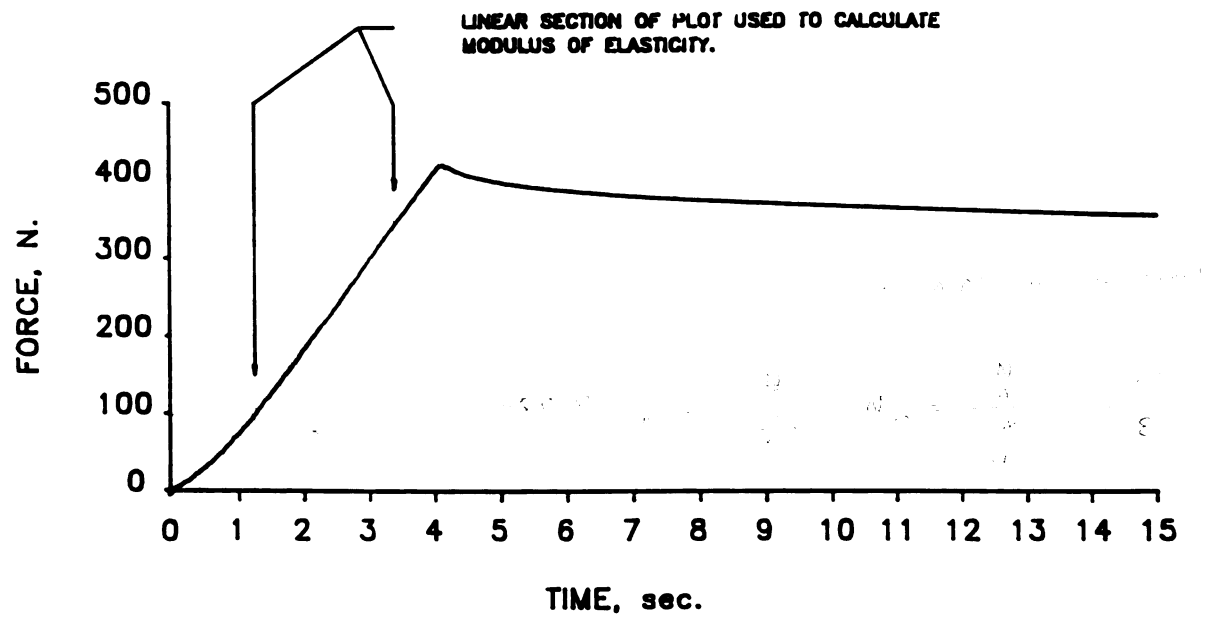


Figure 3.4 Force versus time curve obtained for modulus of elasticity measurement.

3.1.4 Apple Mass Measurement

Apple mass was measured by an Ohaus, Brainweight B1500D electronic scale with a range of 0-1500 grams. Measurements were recorded to 0.1 gram.

3.1.5 Apple Storage

The apples used in this study came from either controlled atmosphere storage or were freshly picked. During experimentation, apple batches were stored in boxes inside a cooler at a temperature of 1° C.

3.2 Procedures

The purpose of the experimentation was to provide quantitative information on the acoustic impulse response of apples and pertinent apple physical properties for use with the model given in Equation [41]. This model would be used as a predictor of flesh firmness. Measured values of flesh firmness would provide a comparison with predicted firmness. Abbott (1968) & Finney (1971) have shown that natural frequencies of apples are dependent on mass, as indicated by Equation [41]. Other variables that the model indicates as being important are density, and Poisson's ratio. The effect of skin stiffening or the non-homogeneous composition of an apple cannot be predicted by this model. Experimental procedures to minimize skin stiffening, without altering the apple mass, was achieved by multiple cuts of the skin surface.

Four batches of apples were used for experimentation.

The number of apples in each batch varied from 50 to 120. Subgroups of apples were taken from each batch and tested periodically. Testing was spread over a period of approximately 6 weeks, for each batch, to allow a measurable drop in firmness within the batch. Modulus of elasticity and resonant frequency measurement techniques differed somewhat between batches. Specific techniques are given for each batch.

3.2.1 Controlled Atmosphere (CA) Rome Beauty

Subgroups of 20 apples for a total of 120 apples were tested on each of the dates given below. Measured variables included the acoustic impulse response, test mass and Magness-Taylor firmness readings. The subgroups were tested on the following dates: 11/2/87, 11/9/87, 11/16/87, 11/23/87, 11/30/87, 12/7/87. The total number of results from the apples tested was 118.

Natural frequency measurements were conducted as outlined in section 3.1.1. Test mass was determined just prior to impulse testing. Magness-Taylor firmness was also determined as outlined section 3.1.3. Five to seven readings, depending on the size of the apple, were taken along the equator. The average value of these readings was used as an indication of apple flesh firmness.

3.2.2 Controlled Atmosphere (CA) Law Rome

Subgroups of 10 apples were tested on the dates given below. Measured variables included the acoustic impulse response, test mass and the modulus of elasticity. The subgroups of apples were tested on the following dates: 2/2/88, 2/9/88, 2/14/88, 2/21/88, 3/7/88. A total of 50 apples were tested.

Elastic modulus was determined as outlined in section 3.1.2 with four cylindrical specimens taken from the cheek of each apple and separately tested, (See figure 3.5 for orientation). Specimen size was 15.9 mm in diameter and 25.4 mm long. Specimens were obtained using a thin tubular cutting knife and specimen holder as shown in figure 3.6. The tube was pushed by hand into the top of the apple traversing to the bottom of the apple. The knife had an outside bevel at the cutting edge. Care was taken not to rotate the knife while cutting as specimens could shear from torsion. To obtain parallel flat surfaces at the ends, the specimen was placed in the holder which was made from a 25.4 cm, plate plexi-glass with a hole drilled through it, see figure 3.6. The hole diameter was the same as the specimen diameter. A razor blade was used to cut the ends with the flat surfaces of the plexi-glass used as a guide.

The modulus of elasticity values obtained from the four specimens were averaged and used as an indicator of the apple's flesh strength.

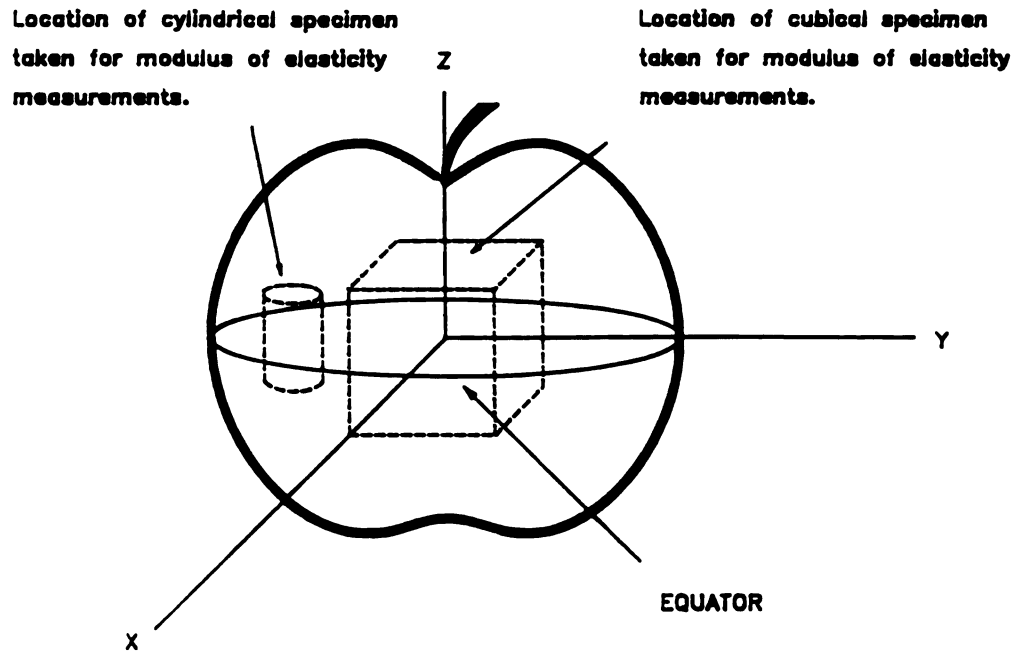


Figure 3.5 Relative location with respect to the apple where specimens were obtained for modulus of elasticity measurement.

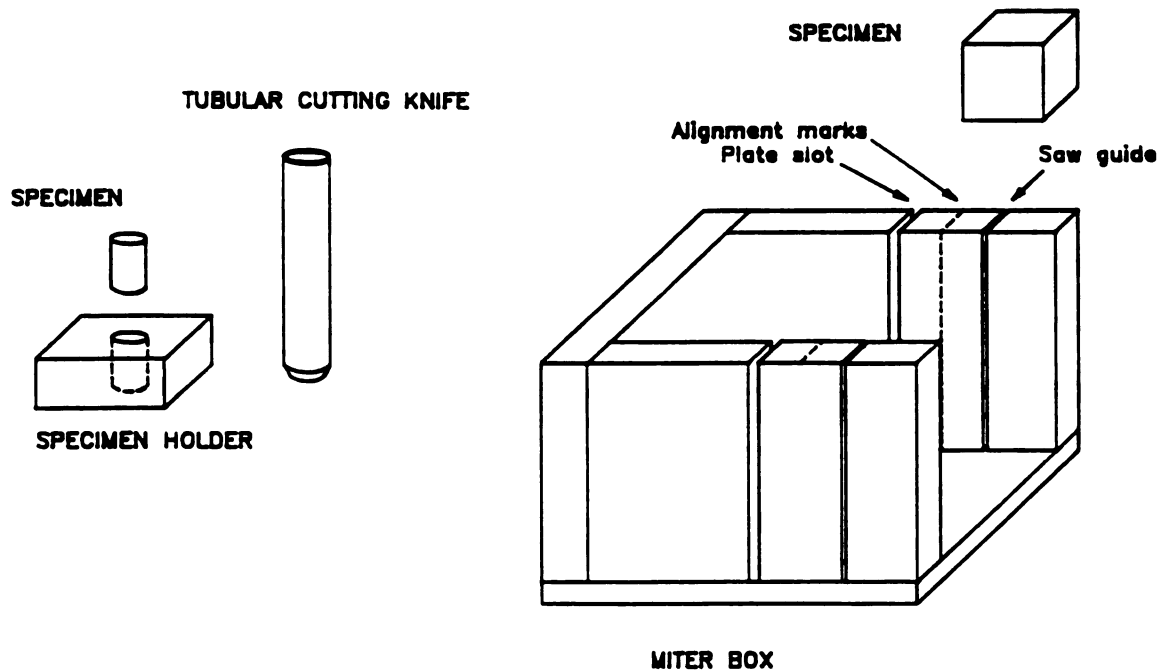


Figure 3.6 Apparatus used to obtain the specimens.

Sixteen CA Law Rome apples were measured for natural frequency and mass on the same test dates as the above CA Law Rome apples. Resonant frequency behavior for the apples as a function of time and aging was thus observed.

3.2.3 Paula Red

Subgroups of 10 apples for a total of 70 apples were tested on the seven dates given below. Measured variables included the acoustic impulse response, test mass, density and the modulus of elasticity. The subgroups of apples were tested on the following dates: 9/2/88, 9/7/88, 9/12/88, 9/17/88, 9/22/88, 9/27/88, 10/3/88.

The natural frequency measurements were conducted as outlined in section 3.1.1 with the following addition: apples were tested with the skin intact and with the skin cut by a multiple-bladed knife. The cuts were made laterally and longitudinally over the surface of the apple, approximately 0.5 mm deep and separated by 5 mm. The purpose of these cuts was to negate the stiffening effect that the skin had on the apple. The mass of each apple was measured immediately after harvest and apples were grouped into batches of 10 with each batch having the same approximate average weight. Average weights at testing for each group ranged from 203.39 to 207.37 grams, with a standard deviation that ranged from 7.37 to 11.85 grams. The purpose of controlling weights was to establish apple groups that would have similar core-to-flesh ratios and shapes. Mass was again measured, for each apple, prior to its acoustic response and

elastic modulus measurement.

The elastic modulus was determined as outlined in section 3.1.2. One cubical specimen was taken from the center of each apple and separately tested. Figure 3.5 shows the orientation of the cubical specimen with respect to the apple. The specimen size consisted of a 38 mm cube which included the core of the apple with the axis of the core emerging from opposite faces of the cube at its center. Specimens were cut from the apple using a fine blade hack saw and a specially constructed miter box as shown in figure 3.6. The saw was used for cutting, as initial attempts with a knife did not produce consistent flat surfaces. Apples were set upright in the box with the core being aligned as close as possible to centering marks, to obtain symmetric specimens with respect to the core. A side of the apple was initially cut to form a flat surface which would also be a side of the cube. The apple was then placed in the box resting on this flat surface with the core again aligned with the marks. A second side was cut which was perpendicular to the first. A third cut was made with the apple resting on a flat side with the second flat surface against the wall of the miter box. A plate inserted into the box served as a guide for the remaining cuts. Specimens were placed in the compression tester with the core horizontal to the compression plates. Specimens were tested at a cross-head speed of 0.05 cm/s, and loaded up to a force of approximately 400 N. Density of each apple was determined by

water displacement prior to natural frequency and elastic modulus determination.

3.2.4 Golden Delicious

Subgroups of 10 apples for a total of 60 apples were tested on the six dates given below. Measured variables included the acoustic impulse response, test mass, density and the modulus of elasticity. Subgroups of apples were tested every six days on the following dates: 10/8/88, 10/13/88, 10/18/88, 10/23/88, 10/28/88, 11/3/88.

Experimental procedures were the same as for the Paula Red with the following exceptions:

1. 10 reference apples were measured for their acoustic impulse response immediately following picking and on each test date listed above.
2. The standard deviation of mass for each subgroup was increased to a range of 23.97 to 39.35 grams for an average mass for each subgroup from 196.5 to 201.2 grams.

IV RESULTS

4.1 Magness-Taylor Firmness and Model Predictions

Tests conducted on CA Rome Beauty apples utilized Magness-Taylor firmness readings primarily because of the acceptance of this measurement in the industry. Figure 4.1 illustrates the results of Magness-Taylor values versus the predicted modulus of elasticity as defined by Equation [41]. The model assumed the compressional, S_{01} , mode of the apple (vibration in a radial direction only) referred to henceforth, as the breathing mode. Although the exact mode was not determined, an examination of Equation [41] reveals that for any assumed mode, and for a constant Poisson's ratio, the values predicted are linearly related. Poisson's ratio was assumed to be 0.3 for all apples. Apple density was also assumed to be constant in the model as reasonably mature apples have only moderate variations between apples. A value of 800 kg/m^3 was used. The coefficient of determination, r^2 , from linear regression of Magness-Taylor firmness on the predicted modulus of elasticity values is 0.265, ($N=118$). Thus 26.5% of the variability in the predicted modulus of elasticity can be explained by a linear relationship.

Clark (1973) suggested that certain modes of vibration are effected by localized material properties, ie. a pure

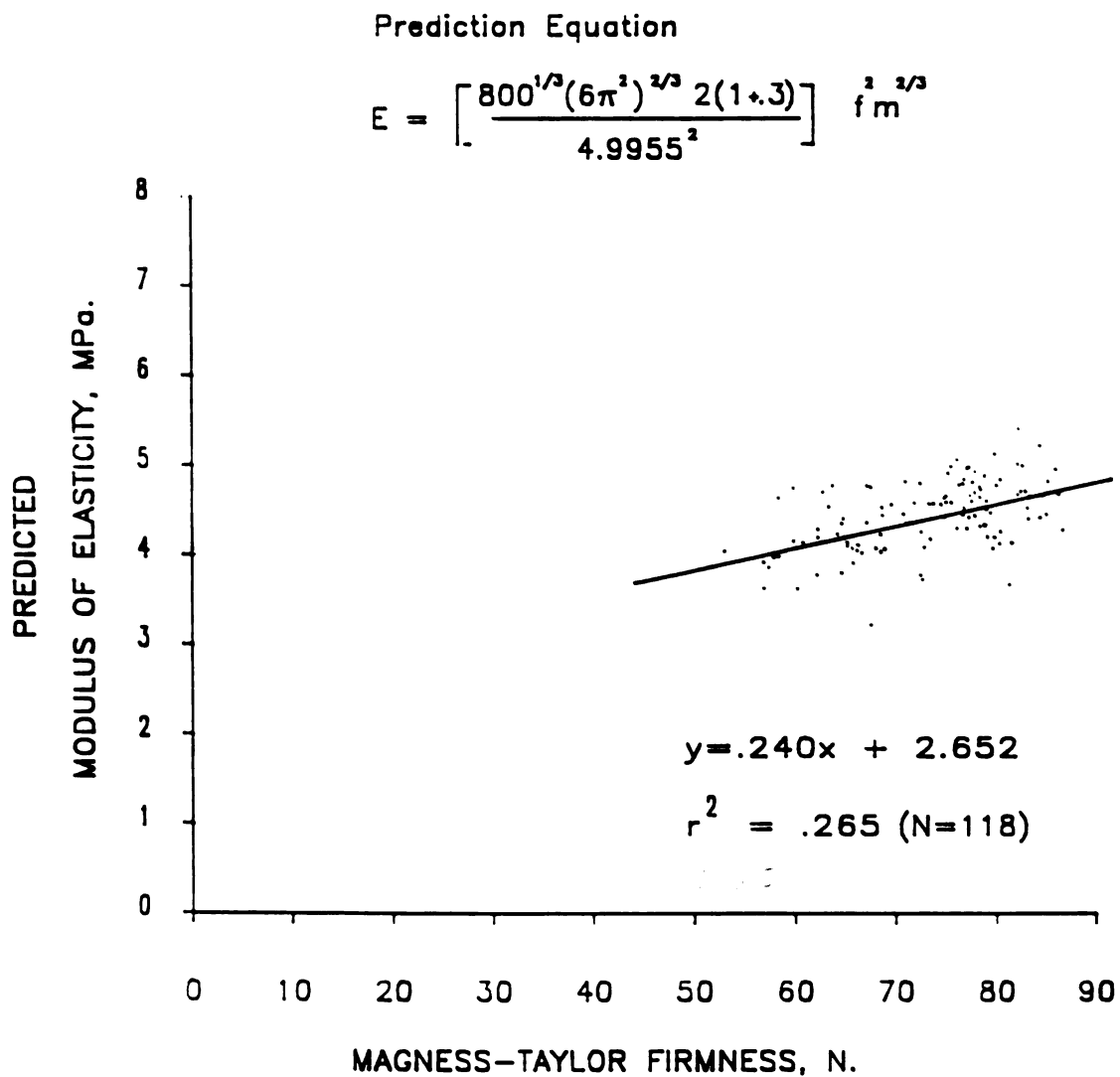


Figure 4.1 Predicted modulus of elasticity versus measured Magness-Taylor firmness for CA Rome Beauty apples.

torsional vibration of a low-order mode would be less influenced by the material properties near the core of the apple than at the circumference. As indicated by the low correlation of these results, one might suspect that Magness-Taylor properties are not directly influencing the modes of vibration induced by the methods used in this research.

4.2 Elastic Modulus of Flesh and Model Predictions

Tests on CA Law Rome apples were conducted similar to CA Rome Beauty apples with the exception that apple properties were determined by compression tests, which yield modulus of elasticity, rather than Magness-Taylor firmness. This provided a more analytical approach than could be achieved from firmness readings. Measurement of modulus of elasticity from compression testing is a non-destructive measurement of the elastic properties of the apple flesh as opposed to Magness-Taylor testing which involves shearing and crushing of the apple flesh. Resonant vibrations in an elastic medium are dependent on the mediums' elastic properties and thus modulus of elasticity should provide a better determination of the flesh strength for comparison with model predictions. Predictions of the modulus of elasticity can be directly compared to the measured values which would help indicate the mode of vibration induced. Modulus of elasticity was evaluated for each apple using a cylindrical sample from the cheek as outlined in the experimental procedures section. Figure 4.2 shows predicted

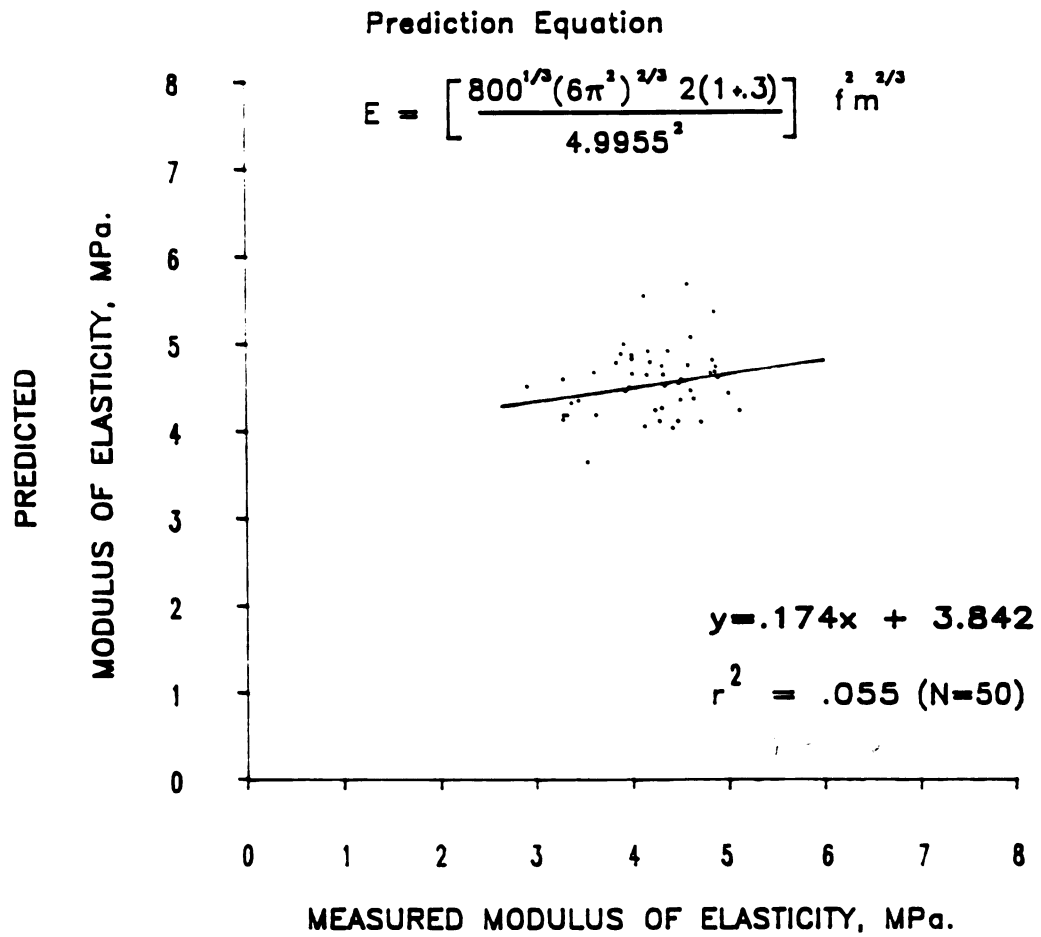


Figure 4.2 Predicted versus measured modulus of elasticity for CA Low Rome apples.

modulus of elasticity of the apple versus its measured value. The breathing mode, a Poisson's ratio of 0.3 and a density of 800 kg/m^3 is assumed for the model. The coefficient of determination, r^2 , from the regression of measured data on predicted modulus of elasticity for this case is 0.055, ($N=50$). The low coefficient of determination obtained contradicts the above stated argument for using this type of measurement for comparison with the model predictions. As will be seen in section 4.3, using specimens that include the core and some flesh for modulus of elasticity measurements, regression with predicted values are much improved.

Sixteen CA Law Rome apples from the same source as the above tested apples were measured concurrently for their impulse response. Resonant frequencies of these apples with respect to time are shown in figure 4.3. Frequencies decreased with age, in general, except for 3 cases.

4.3 Core-Flesh Elastic Moduli and Model Predictions

Due to the non-homogeneous composition of an apple and the assumption that it will vibrate in a breathing mode, core elastic modulus could have a significant effect on vibrational frequency. Measurements by Abbott et al. (1968 a) showed flesh strength to increase then decrease toward the center of the apple. This might be expected due to the presence of seeds and cavities. Core strength was also found by Abbott (1968 a,b) to be slightly less than flesh strength and significantly less than skin strength.

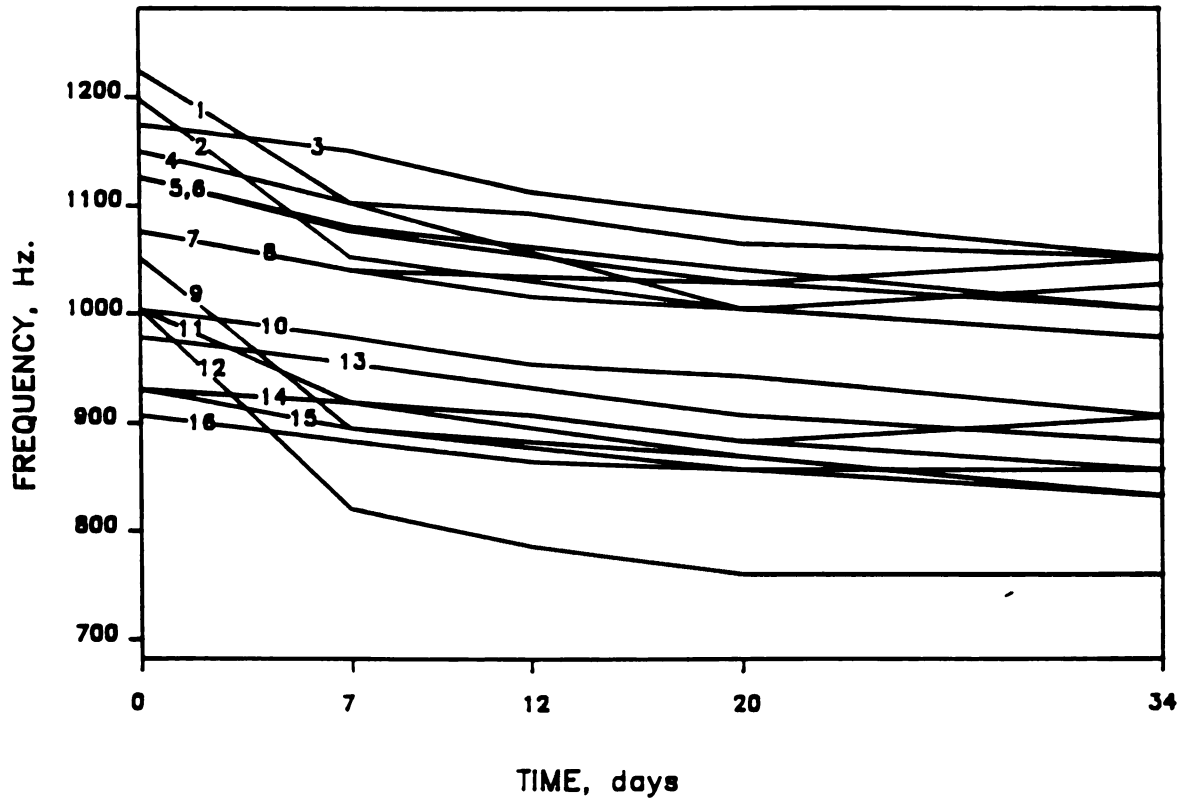


Figure 4.3 Drop in peak frequency versus time of 16 CA Low Rome Apples.

Results that included core strength in the modulus of elasticity measurements and the effect of skin stiffness were conducted on Paula Red and Golden Delicious apples. In all the predicted values of modulus of elasticity the model assumed the breathing mode.

Tests on Paula Red apples were conducted as outlined in Chapter 3. Figure 4.4 shows predicted versus measured modulus of elasticity. The model incorporated measured density, mass, an assumed Poisson's ratio of 0.3, and the resonant frequency of the apple with the skin intact. The coefficient of determination from the regression of measured on predicted modulus of elasticity is 0.774, (N=70).

The impulse response of apples measured with the skin cut was always less than that with skin intact (uncut). It was observed that cutting the skin dropped the resonant frequencies to stable values beyond which further cutting had no effect. Resonant frequencies obtained from cut and uncut apples are presented in the appendix. The purpose of cutting was to better approximate the elastic sphere model. Figure 4.5 shows predicted versus measured modulus of elasticity for the same apples used to obtain figure 4.4 but with the skin cut. The model uses an assumed Poisson's ratio of 0.3, the measured density and the measured mass. Compared to the uncut apple, cutting the apple had little effect on the coefficient of determination, $r^2 = 0.798$, (N=70), derived from the regression of measured modulus of elasticity data. The model employed in figures 4.4 and 4.5

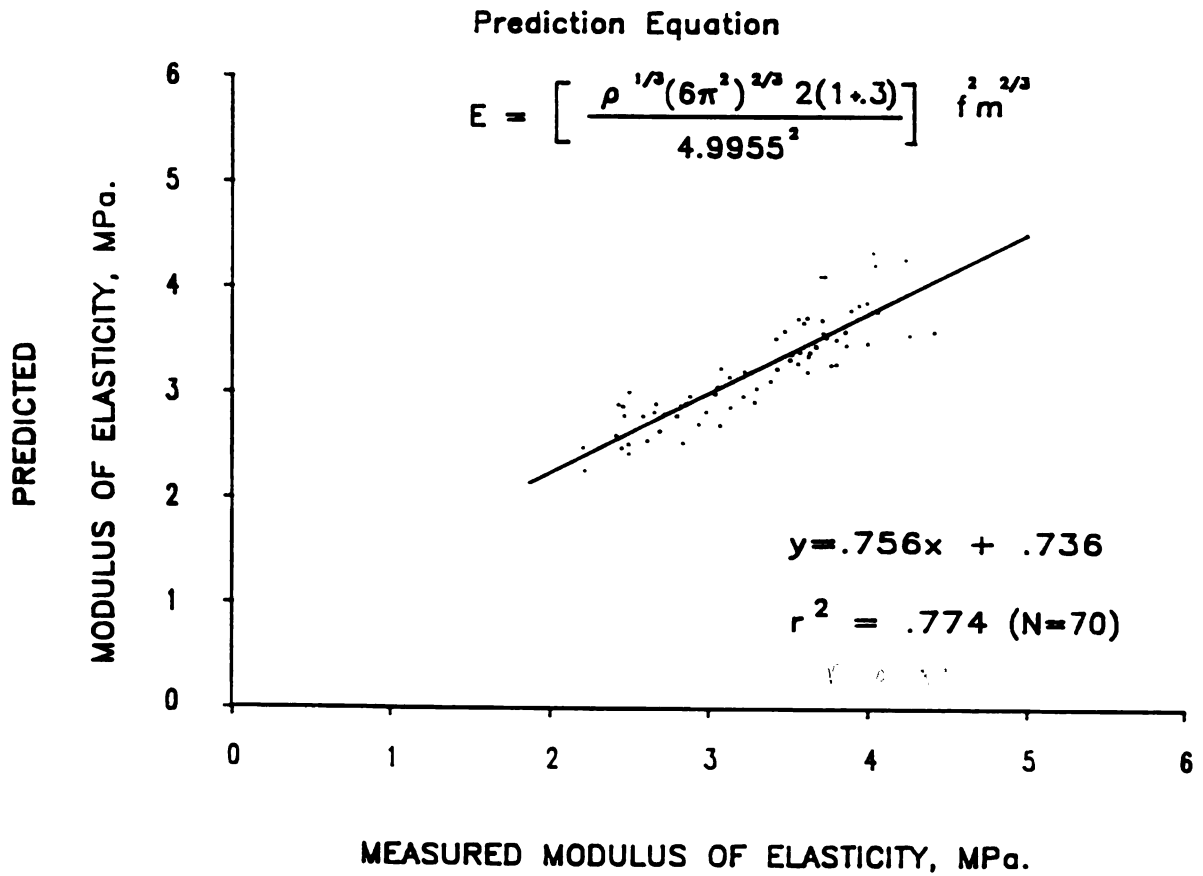


Figure 4.4 Predicted versus measured modulus of elasticity for Paula Red apples .

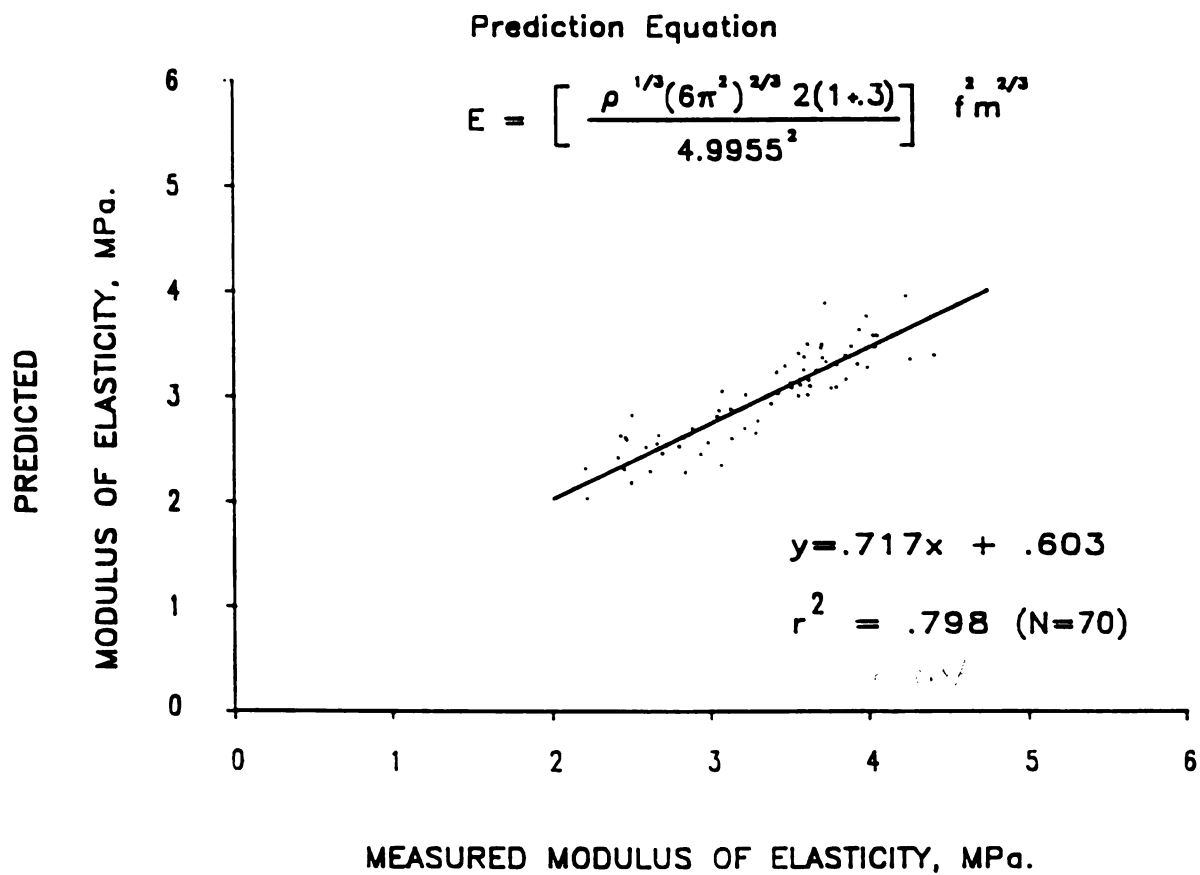


Figure 4.5 Predicted versus measured modulus of elasticity for Paula Red apples.

uses the measured density of individual apples. By assuming a constant density of 770 kg/m^3 the moduli of elasticity predicted by the model were calculated: these and the corresponding measured values are shown in figure 4.6. The constant density value used was the average value of all apples tested in this batch. The coefficient of determination is 0.803, ($N=70$). The model also uses the uncut apple's peak resonant frequency, a Poisson's ratio of 0.3 and the apple mass.

Frequency was considered as the sole predictor of firmness. Peak frequencies of the uncut apples were squared and regressed with the measured modulus of elasticity for the Paula Red apples. These results are shown in figure 4.7. The coefficient of determination is 0.769, ($N=70$).

Golden Delicious apples tested in the same manner as the Paula Red apples displayed similar coefficients of determination from similar analyses. Figure 4.8 shows the regression of measured on predicted modulus of elasticity. The model used measured density, the uncut resonant frequency, an assumed Poisson's ratio of 0.3 and the apple mass. The coefficient of determination for this case is 0.793, ($N=60$). The corresponding results from Paula Red apples analyzed in a similar manner was shown in figure 4.4.

Results for cut Golden Delicious apples are shown in figure 4.9. These results, with a coefficient of determination of 0.786, ($N=60$), were obtained in a similar manner to those for the Paula Reds (figure 4.5).

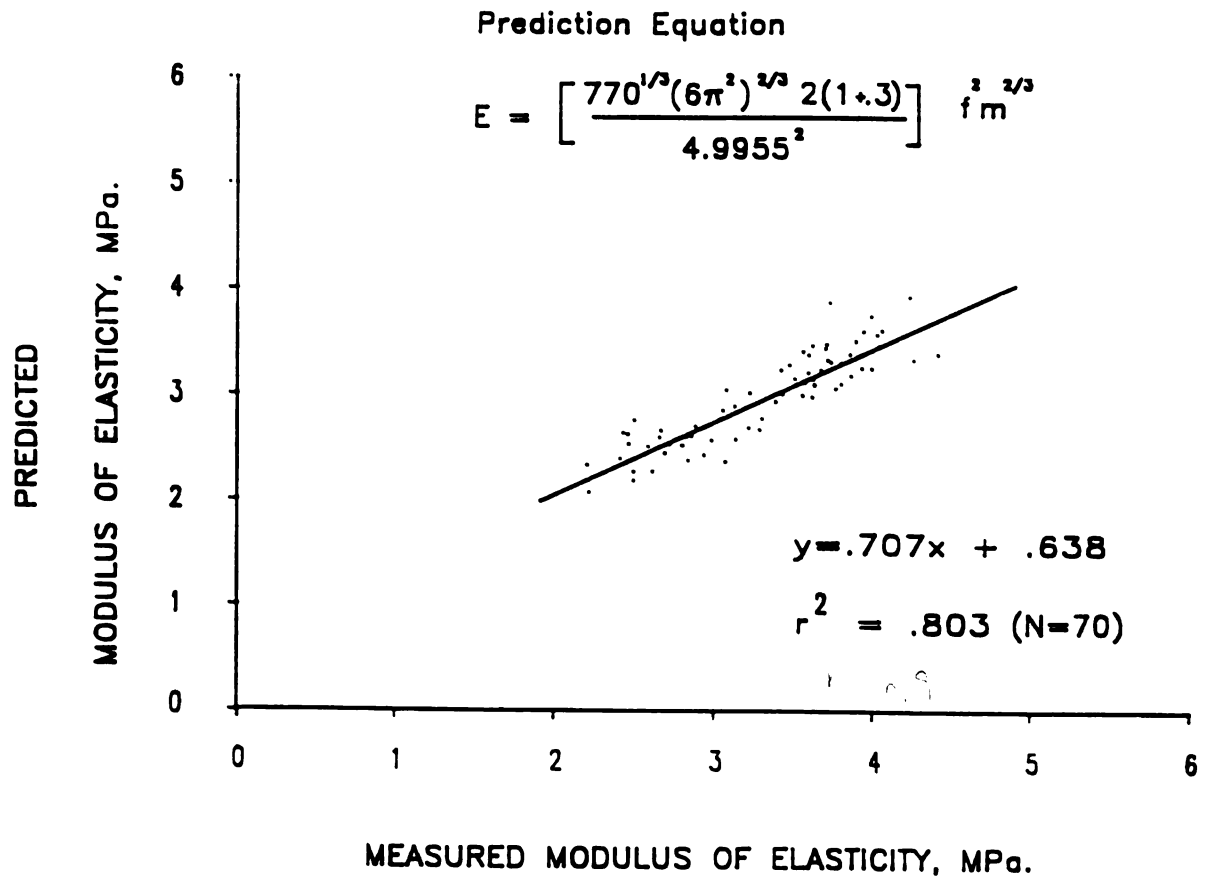


Figure 4.6 Predicted versus measured modulus of elasticity for Paula Red apples.

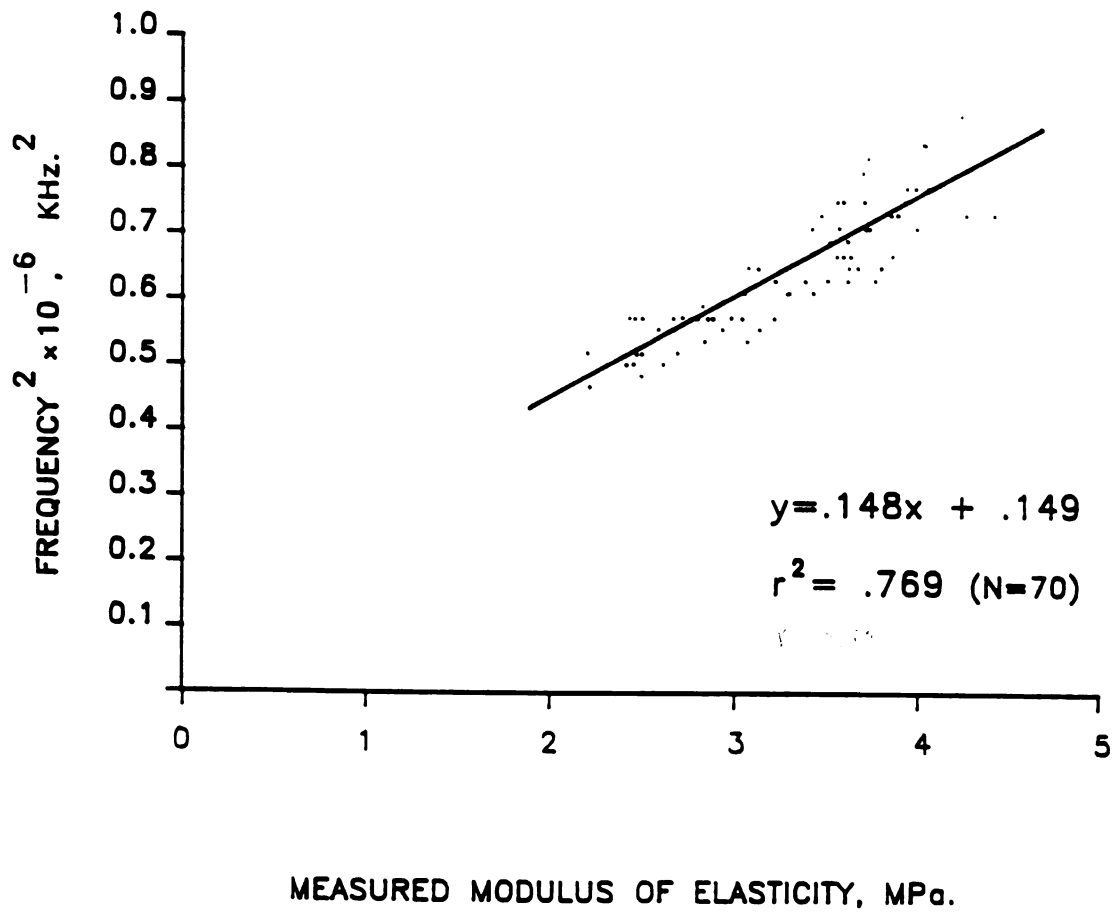


Figure 4.7 Frequency squared versus measured modulus of elasticity for Paula Red apples.

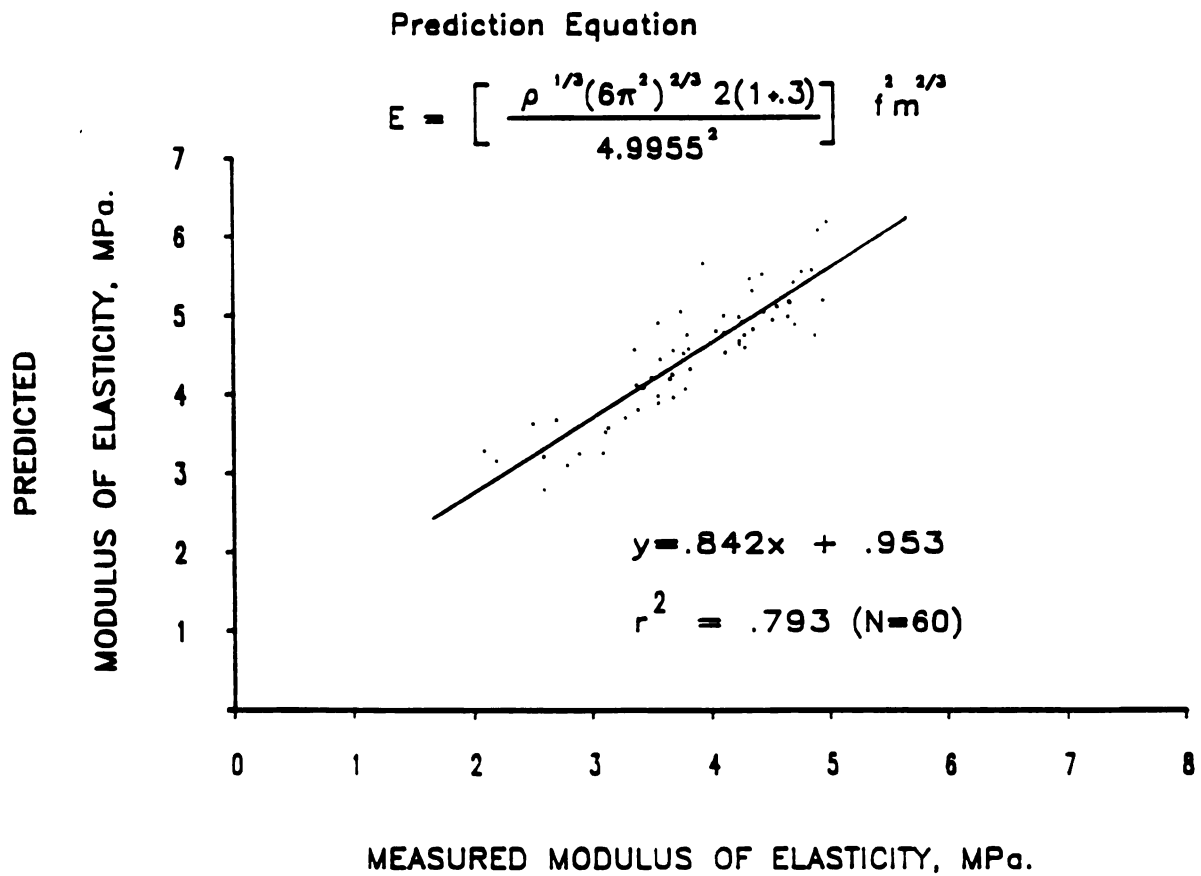


Figure 4.8 Predicted versus measured modulus of elasticity for Golden Delicious apples.

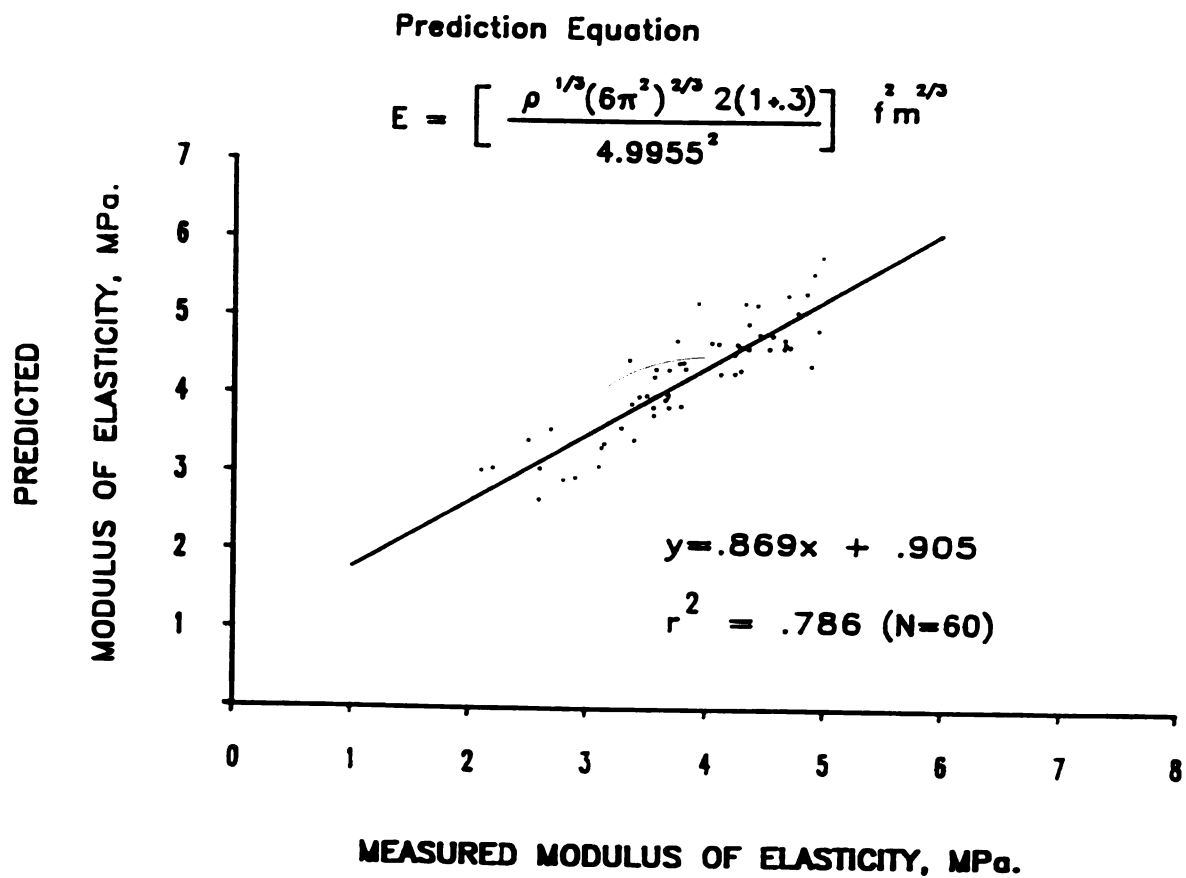


Figure 4.9 Predicted versus measured modulus of elasticity for Golden Delicious apples.

Figure 4.10 shows regression results ($r^2=0.790, N=60$) for Golden Delicious apples with the model using a Poisson's ratio of 0.3, the uncut apple's resonant frequency, apple mass and an assumed constant density. The constant density value used was 812 kg/m^3 which is the average density of the apples in the batch. Results for Paula Red apples, for a constant density assumption, are shown in figure 4.6.

Peak frequencies of the uncut Golden Delicious apples were squared and regressed with the measured modulus of elasticity, as shown in figure 4.11. The coefficient of determination is 0.544, ($N=60$).

The change, with respect to time, of resonant frequencies for ten Golden Delicious apples is shown in figure 4.12. These apples were picked from the same orchard at the same time as the Golden Delicious apples discussed above and have the same test dates (except for the first date). The first test date in figure 4.12 was the date the apples were picked. The impulse response of these ten apples were recorded in the orchard. Data were recorded on cassette tape and played back to the Analogic 6000 oscilloscope for analysis. Subsequent measurements were taken in the laboratory.

4.4 Summary of Regression Results

Table 4.1 is provided for easy comparison of the regression results shown in the previous figures. These results show that the model is not a good predictor of Magness-Taylor firmness (CA Rome Beauty apples) or modulus

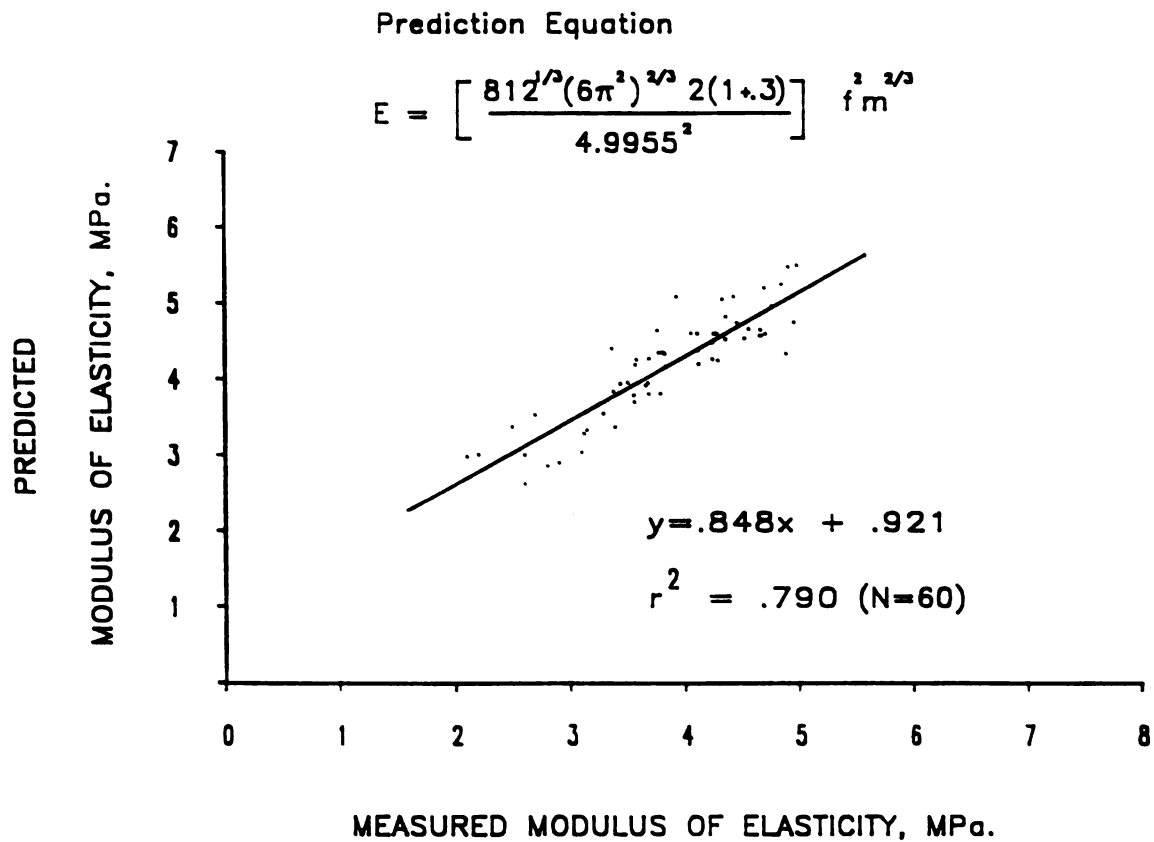


Figure 4.10 Predicted versus measured modulus of elasticity for Golden Delicious apples.

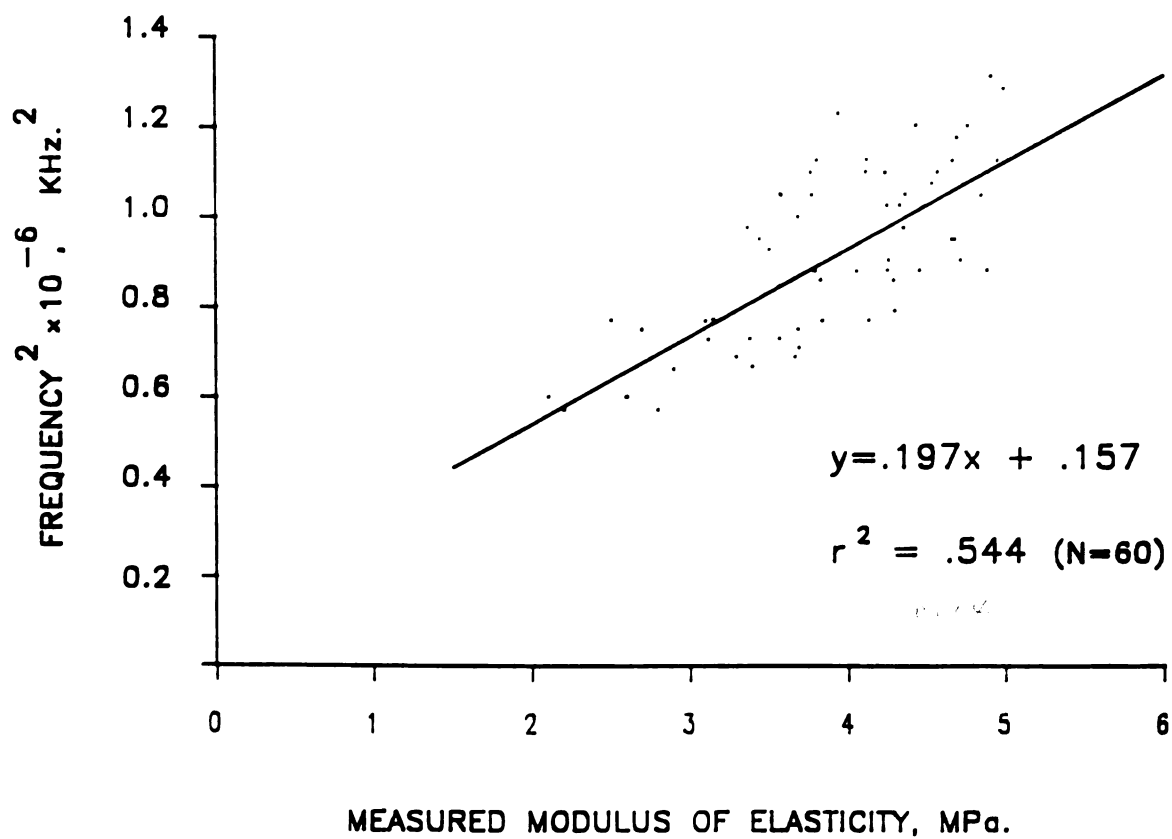


Figure 4.11 Frequency squared versus measured modulus of elasticity for Golden Delicious apples.

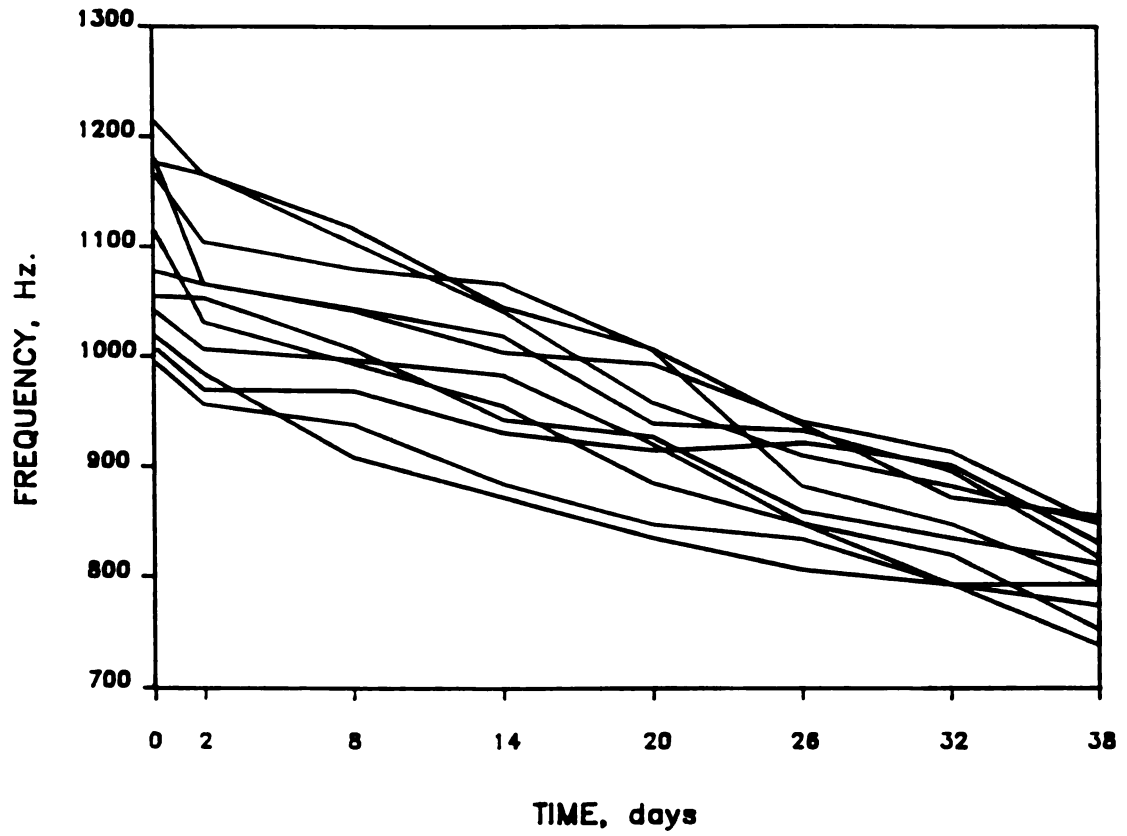


Figure 4.12 Drop in peak frequency versus time for 10 Golden Delicious apples.

of elasticity of the apple flesh (CA Law Rome apples) as indicated by the low coefficients of determination (0.265 and 0.055 respectively in table 4.1). As mentioned previously Magness-Taylor values are obtained by shearing and crushing the apple flesh. This might be compared to Brinell hardness testing of metals for which hardness values do not necessarily have linear relationships with the modulus of elasticity of the metals. Natural vibration of an apple would most likely involve flesh stresses well within the yield point of the flesh while Magness-Taylor values are obviously measuring apple flesh strength near or beyond the yield point as opposed to the flesh strength predicted by the model.

Table 4.1 Regression results from the study.

Result	r^2	N	Variables in model	Firmness measurement	Apple Variety
1	0.265	118	m, f1	Magness-Taylor	CA Rome Bty.
2	0.055	50	m, f1	M.of E. (cylinder)	CA Law Rome
3	0.774	70	m, p, f1	M.of E. (cube)	Paula Red
4	0.798	70	m, p, f2	M.of E. (cube)	Paula Red
5	0.803	70	m, f1	M.of E. (cube)	Paula Red
6*	0.769	70	f2	M.of E. (cube)	Paula Red
7	0.793	60	m, p, f1	M.of E. (cube)	G. Delicious
8	0.786	60	m, p, f2	M.of E. (cube)	G. Delicious
9	0.790	60	m, f1	M.of E. (cube)	G. Delicious
10*	0.544	60	f2	M.of E. (cube)	G. Delicious

m = apple mass

p = apple density

f1 = resonant frequency with the apple skin uncut

f2 = resonant frequency with the apple skin cut

M.of E. = modulus of elasticity(type of specimen)

* Squared value of frequency was used as predictor.

Cylindrical specimens used to determine modulus of elasticity were small in comparison to the cubical specimens and were more difficult to prepare. Because of this the modulus of elasticity values measured using the cylindrical specimens were increasingly prone to experimental error. Specific reasons for this were:

(1) Specimens were physically harder to hold.

(2) Some specimens had to be discarded because: they were sheared in half, they showed visible defects of the cut surface or the specimens were not straight when taken from the plug (caused by either internal stress relief or improper cutting). Although these defective specimens were discarded, the specimens that were used may have been structurally altered by the cutting process.

(3) Specimens contained varying amounts of vascular material (which is significantly different in strength than the surrounding flesh).

Modulus of elasticity values from cylindrical and cubical specimens are of the same magnitude and one would expect good correlation between the two. Despite this the correlation results using the cylindrical specimens are quite low whereas for cubical specimens the model shows a good ability to predict modulus of elasticity.

Entries 3-5,7-9, from Table 4.1 for Paula Red and Golden Delicious apples show that the model has good modulus of elasticity prediction ability. Whether the uncut or cut apple peak frequency is used in the model, correlation

results do not change appreciably (results 3,4 and 7,8 in Table 4.1). This is also true if measured density is used rather than an assumed density (results 3,5 and 7,9 in Table 4.1).

The coefficient of determination obtained from using the squared frequency as the firmness predictor (result 10 in Table 4.1) for the Golden Delicious apples is much lower than for the Paula Red apples (result 6 in Table 4.1). This was expected since the standard deviation of the mass for Golden Delicious apples was greater than for the Paula Reds and implies the functional dependence the resonant frequency has on mass, as indicated in Equation [41].

In all the above cases the breathing mode was the assumed primary vibrational mode of the apple. Different modes would yield the same correlation results assuming a constant Poisson's ratio. Reasons for using the breathing mode were:

- (1) The measured values of modulus of elasticity were close to those predicted by the model
- (2) The breathing mode is the lowest-order mode of pure compression.
- (3) Torsional modes are not likely to be induced because of the method of excitation used.
- (4) The possibility of mixed modes exists, but higher-order modes would have to be used to obtain values of modulus of elasticity which are close to the measured values.

Modes which would give equivalent modulus of elasticity values would be the S_{21} and S_{40} modes.

V CONCLUSIONS

The fundamental objective of this research was to determine if the acoustic impulse response of an apple could be used to determine tissue firmness. The spherical resonator model, which utilized the response spectrum to predict modulus of elasticity, had good correlations with the measured modulus of elasticity of tissue that included the core. Less impressive correlations were obtained when predicted modulus of elasticity was regressed on Magness-Taylor firmness or the measured modulus of elasticity of flesh specimens. A list of conclusions follows.

1. The techniques used in this research for obtaining the acoustic impulse response of an apple provide an easy and reliable means of identifying the vibrational characteristics of the apple.

2. The measured modulus of elasticity of apple specimens that included the core and apple flesh of the apple had good correlation, $r^2 > 0.773$ ($N=60,70$), with the modulus of elasticity predicted by the spherical resonator model for Paula Red and Golden Delicious apples.

3. The measured modulus of elasticity of apple specimens that were taken from the cheek of the apple did not correlate well with the modulus of elasticity predicted by the spherical resonator model, $r^2=0.055$ ($N=50$), for CA Law

Rome apples.

4. The Magness-Taylor firmness of an apple did not correlate well with the modulus of elasticity predicted by the spherical resonator model, $r^2=0.265$ ($N=118$), for CA Rome Beauty apples.

5. Skin stiffening of the apples were apparent from the higher resonant frequencies obtained for uncut apples compared with the resonant frequencies for the cut apples.

6. Neither the use of the peak frequency for cut apples, nor the assumption of a constant density in the spherical model appreciably changed the ability of the model to predict modulus of elasticity for Paula Red and Golden Delicious apples.

7. The techniques used in this research provide a non-destructive method for firmness evaluations of apples. The method of impulsive excitation and resonant analysis could be used in research where non-destructive firmness measurements may be necessary.

VI RECOMMENDATIONS FOR FUTURE RESEARCH

Based on results and experience of this research, the following recommendations for future research are suggested:

1. Improved measurement techniques to more accurately measure the firmness of the flesh part of the apple need to be developed. Measurement techniques used to determine the modulus of elasticity of the cylindrical apple specimens could be improved by using larger specimens and better cutting techniques. Better samples should provide better correlations with the model predictions.

2. Incorporation of the deviation of the apple shape from a true sphere should result in a more accurate model for the prediction of the modulus of elasticity. This was not done for the reported research except for some minor experiments with an elastic medium which was formed into an apple shape.

3. Determination of the true vibrational mode of an apple when excited by an impulse would provide a more realistic description of the true apple characteristics. A technique which could be tried is the strategic placement of microphones near the surface (or accelerometers on the surface) of the apple and the observation of phase relationships of the vibrating surface.

4. Due to the sensitivity of the model to frequency, sampling techniques of the impulse response could be changed to increase the resolution of the FFT and thus a more precise estimate of the resonant frequency would result.

5. A thorough understanding of the variations of tissue strength within an apple needs to be developed. Results from this research show that the modulus of elasticity of specimens that include the core can be reasonably predicted by the model. If a relationship exists between core strength and flesh strength the model would be more useful for non-destructive and rapid textural evaluations. Precise sample and measure techniques would require development to determine the modulus of elasticity of small apple specimens.

VII SUPPLEMENTARY EXPERIMENTATION

The purpose of this chapter is to provide to the reader information obtained during the course of this research that is not directly related to the forgoing material but does provide additional information concerning impulse techniques and signal analysis for firmness determination in apples.

7.1 Water As The Acoustic Carrier

Initial acoustic impulse response experiments were tried with the apple and a sealed microphone under water. The purpose of this was to enhance the acoustic energy transfer from the apple to the microphone and thus reduce the striking force required to produce a suitable signal. The procedure employed was similar to that outlined in the experimental techniques section. Apples were allowed to float to expose a surface for striking. Although a significant reduction in the energy required to excite vibrations was achieved and equivalent results were produced in water and air, difficulties were encountered in water due to acoustic noise entering the apple and microphone container. The water environment itself was less desirable to work in from a practical point of view and further studies were conducted in air.

7.2 Signal Noise

The acoustic signal emitted from the apple can be described as a reasonably clean, exponentially decaying periodic signal. In contrast, undetermined sources of noise and relative large DC offsets in the microphone signal would interfere with a frequency spectrum that would clearly define a resonant mode. The Analogic 6000 was incapable of performing signal filtering, thus FFTs were sometimes performed by an IBM AT which could be programmed to enhance the spectral detail.

A primary problem in the spectral display was the relatively large DC component in the spectrum which was sometimes accompanied by significant frequency components in the 60-350 Hz range. The unfiltered signal and its spectrum, obtained from the IBM FFT routine, is shown in figure 7.1. To suppress the DC component, sampled signal values were set to 0 after the primary acoustic signal had decayed significantly. The altered signal is shown in figure 7.2. Signal manipulation in this manner has effectively the same result as initially sampling for a shorter period but padding the end of the signal with zeros to enhance the resolution of the FFT (a technique commonly used with FFTs). The benefit of this can be seen in the FFT of the altered signal, shown in figure 7.2. This sampling technique generally provided enough attenuation in the DC component to make the frequency peak of interest clearly discernible. An alternative method to diminish the DC

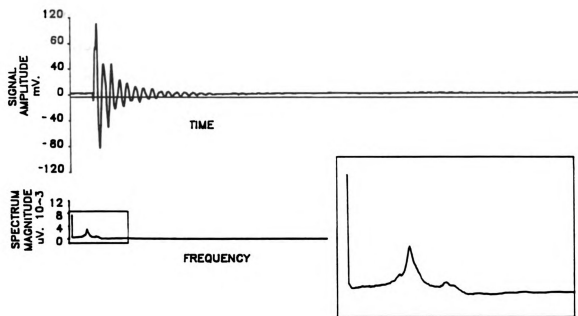


Figure 7.1 Original acoustic signal and its spectrum.

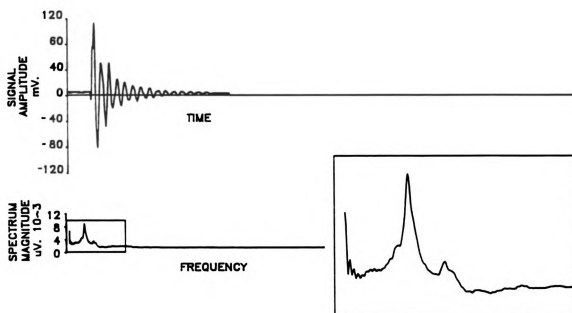


Figure 7.2 DC attenuation of the acoustic signal and its spectrum.

component would be to average the digitized signal values then subtract these from the original signal before performing the FFT. This would require more computation but would eliminate a small aliasing problem caused by zero padding.

Multiple resonant peaks in the FFT were present in a few signals observed and were repeatable for different signals from the same apple. Figure 7.3 shows signals in which this occurs and the spectra obtained by a FFT. Often these peaks were located close to each other and of approximately the same magnitude making it difficult to determine which peak should be used for model predictions of modulus of elasticity. Additional measurements were taken in these cases. The peak with the largest magnitude was always used as the desired resonance in the model. The occurrence of these peaks could be a result of the excitement of multiple resonant modes in the apple.

7.3 Repeatability of the Acoustic Response

No distinguishable difference in impulse response was observed when holding the apple by hand as opposed to suspending the apple by the stem. Variations in striking force as the result of using a hand-held hammer did not result in any detectable difference of spectral content of a signal.

Repeatability of the spectrum for an apple struck along its equator is consistent to within the resolution of the FFT. Peak frequencies determined from the impulse response of five apples, each struck eight times, are shown in

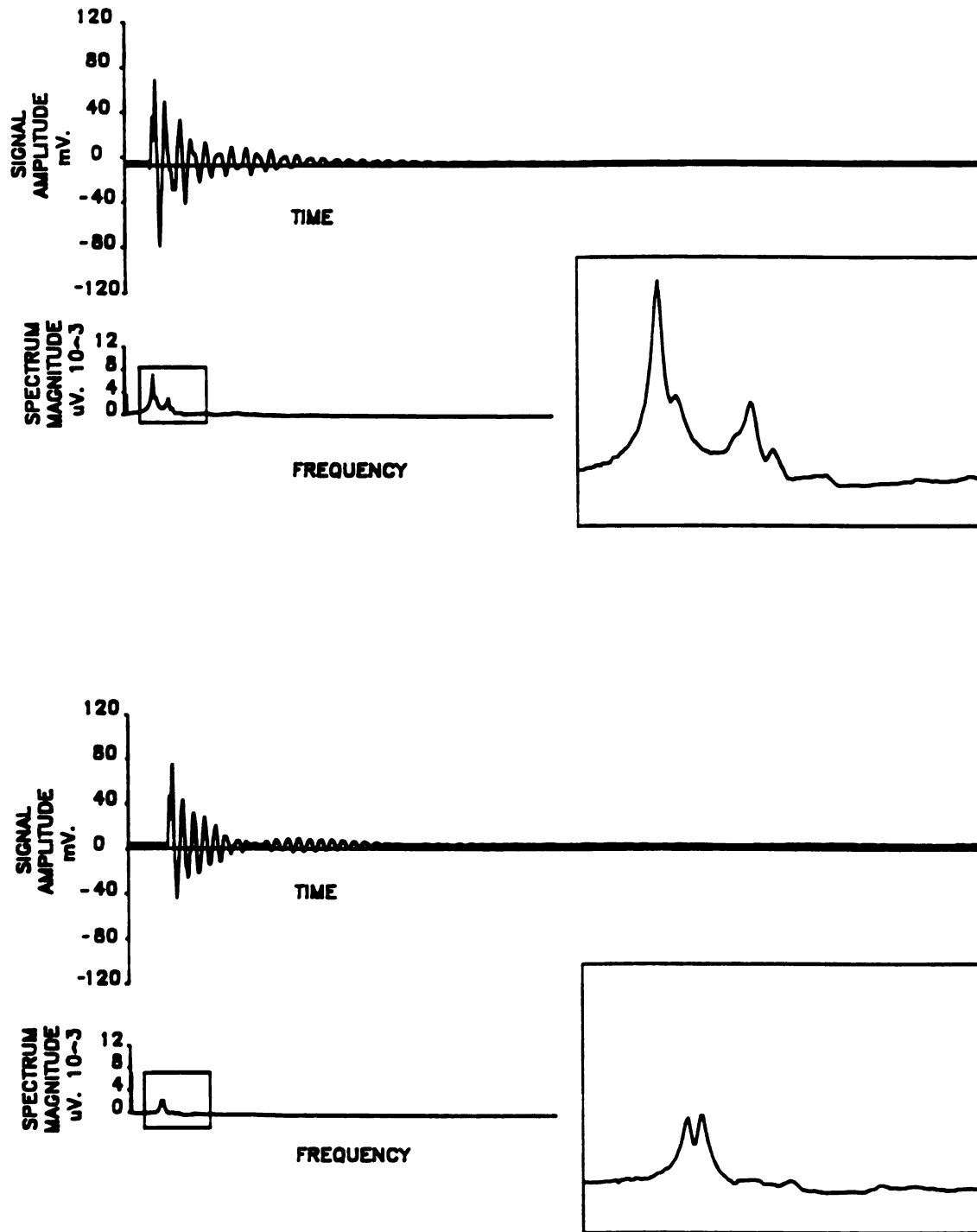


Figure 7.3 Two signals and their spectra displaying multiple resonant peaks.

table 7.1. Peak frequencies for the same apple are consistently reproduced. The receiver/impulse orientation was 180 degrees apart with the apple being struck at the equator.

Table 7.1 Reproducibility of the peak frequency of five apples.

Impulse	Apple				
	1	2	3	4	5
1	1013	903	927	891	964
2	1000	903	927	891	964
3	1013	915	927	891	964
4	1013	903	927	903	964
5	1013	903	927	891	964
6	1013	903	927	891	964
7	1013	903	915	891	964
8	1013	903	927	891	964

To determine the effect the impulse location and receiver orientation have on signal generation, five apples were struck with the orientations shown in figure 7.4. Two replications with random apple orientation were done for each orientation. Results, shown in table 7.2, indicate that there is a change in the peak frequency when the apple is struck on a polar region as opposed to an equatorial region. When the receiver is placed 90 degrees to the impulse direction, the peak frequency lies between the frequencies of the other two orientations with no apparent preference of one or the other.

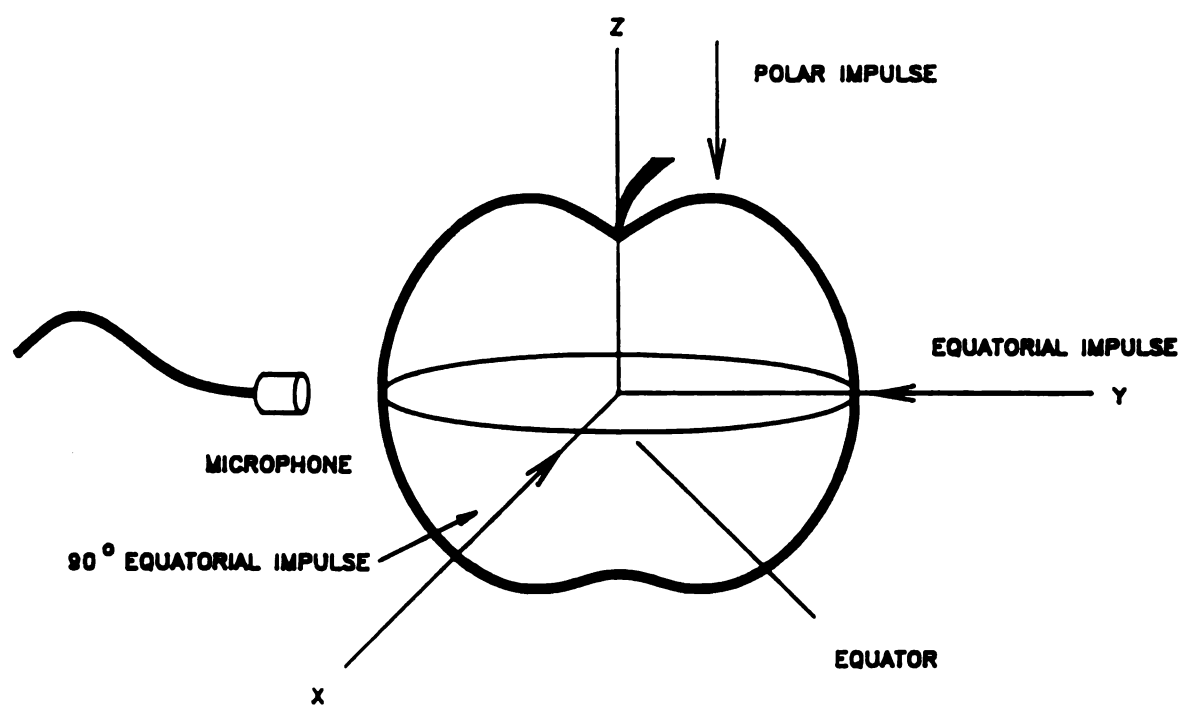


Figure 7.4 Orientation of impulse and microphone.

Table 7.2 Peak resonant frequencies obtained using different impulse locations and receiver orientations for five apples.

Orientation	Apple				
	1	2	3	4	5
Equatorial	854	866	878	854	952
Equatorial	854	866	878	854	939
Polar	878	878	927	927	939
Polar	878	878	927	927	952
90° Equatorial	854	878	878	854	976
90° Equatorial	854	878	878	854	939

7.4 Experimentation with an Elastic Sphere

To verify that the experimental techniques yielded precise results, and to determine the modes of vibration excited, experimentation with a solid rubber ball was conducted and compared with theoretical results based on the vibrating elastic sphere model. The resonant frequencies of a 6 cm diameter rubber ball were measured in a similar manner used for apples. The modulus of elasticity was measured by cutting a cubical sample from the ball and subjecting it to the compression test used for apples.

The spectrum from the ball was similar in appearance as that for an apple with an average peak resonant frequency of 317 Hz from four tests. The weight of the ball was 79.3 gms with a density of 594 kg/m³. Measured modulus of elasticity of a cubical specimen cut from the ball specimen yielded a value of 0.662 MPa. Assuming Poisson's ratios of 0.2, 0.3, and 0.4, and that the ball was resonating in

the breathing mode, the predicted modulus of elasticity of the ball is 0.352, 0.247, and 0.132 MPa respectively. For an oblate-prolate mode of vibration and Poisson's ratios of 0.2, 0.3, and 0.4, the predicted modulus of elasticity is 0.817, 0.880 and 0.940 MPa respectively. These results suggest that the ball is vibrating in the oblate-prolate mode because of the smaller difference between the predicted and measured modulus of elasticity.

To determine the effect that apple shape might have on resonant frequencies, two similar balls, as used above, were cut into the shape of apples. One apple shape was similar to a roundish Rome apple and the other resembled a Golden Delicious shape. Prior to shaping the balls, the resonant frequencies for each ball were determined from the average of four tests. During shaping of the balls into an apple shape, mass was kept constant for both shapes. Results from these tests, shown in table 7.3, indicate that the Golden Delicious shape has a slightly higher resonant frequency than the Rome shape.

7.5 Signals from an Accelerometer

The impulse response of an apple was measured using a Vibrametrics 1009 accelerometer and a microphone for comparison of signal output and spectral content. The accelerometer was attached to the apple surface at the equator, directly opposite the applied impulse and at 90° to the impulse for different measurements. The accelerometer

Table 7.3 Comparison of peak frequencies for two apple shapes and the spherical balls from which they were shaped.

Test #	Ref. Ball 1	Rome¹ Shape	Ref. Ball 2	Red Delicious² Shape
1	317	329	341	366
2	329	329	341	366
3	341	329	321	366
4	317	329	354	366
Average Frequency	326	329	339	366

1 - Rome shape obtained from Ref. Ball 1.

2 - Red Delicious shape obtained from Ref. Ball 2.

was attached with bee's wax for maximum signal transfer. Measurements with the microphone were done as outlined in the experimental techniques section of this report. A second apple was also tested. The three spectra from the response signals (microphone, 180° and 90° accelerometer orientations) are shown for each apple in figure 7.5. with significant frequency components being identified. The spectral signature for both apples are very similar for the same receiver type and orientation.

For simplicity, the frequency peak obtained from the microphone will be referred to as the main frequency, ie. 964 & 817 for apples 1 & 2, respectively. Spectra for the 90° accelerometer orientation has peaks at or near the main frequencies (964 and 830 Hz) for both apples, whereas the 180° orientation does not. Spectral peaks immediately to the right and left of the main frequencies, for accelerometer orientations, occur at similar frequencies. These frequencies may account for the double spikes observed on some spectra obtained from the microphone discussed earlier.

Ratios of the main frequency, obtained from the microphone, to the peak frequencies of the 90° accelerometer orientation are shown in table 7.4. Within the resolution of the FFT, these ratios appear to remain constant for the apples tested.

Considering the modes of vibration being induced in the apple, the oblate-prolate mode is the lowest frequency mode for a sphere and it would seem reasonable that this mode

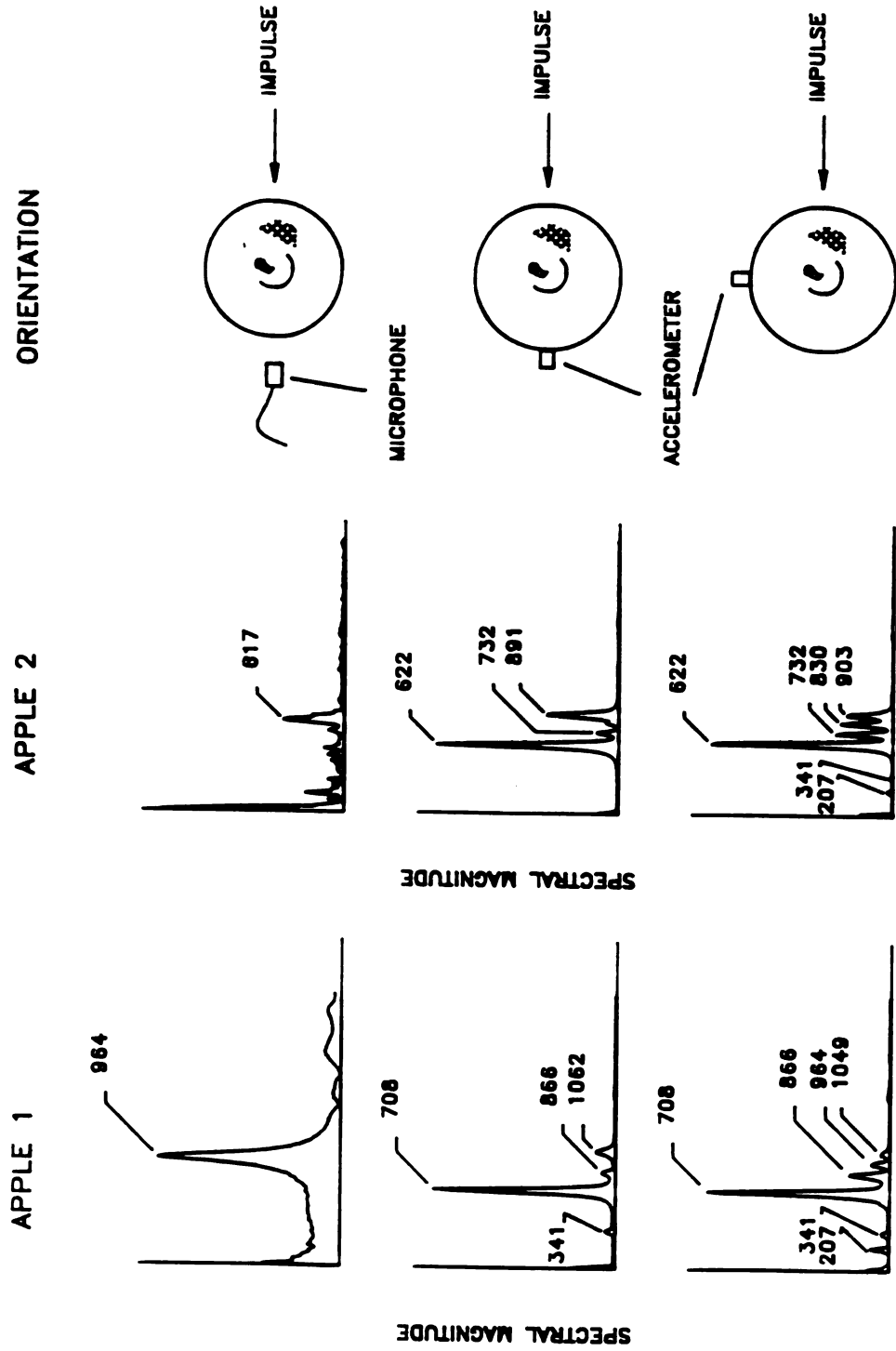


Figure 7.5 Spectra from two apples and the orientation of the receiving device.

Table 7.4 Ratios of peak frequencies
to the main frequency.

Apple 1		Apple 2	
Freq. Hz.	Ratio	Freq. Hz.	Ratio
708	.734	622	.749
866	.898	732	.882
964	1.000	830	1.016
1049	1.088	903	1.088

would be excited by an impulse. If the above frequencies are truly resonant modes of the apple and not resonance of the accelerometer-to-apple connection, then the mode being detected by the microphone (main frequency) is a higher order mixed-mode than the oblate-prolate mode or it is the breathing mode. This conjecture assumes that an apple behaves similarly to a sphere and that pure torsional modes will not be induced to any detectable degree by an impulse.

Lower order mixed modes, $S_{n,1-1}$, are relatively insensitive to Poisson's ratio compared with the breathing mode, S_{01} , and higher order radial modes (refer to figure 2.2). If Poisson's ratio varied significantly between these two apples then the presence of the breathing mode would be indicated by a change in one or all of the above ratios. This was not the case as the ratios did not change. This shows that either the breathing mode is not present or that Poisson's ratio does not change much. The latter case seems more likely.

APPENDIX

Table A1. Data obtained from CA Rome Beauty apples.

Apple Mass kg.	Peak Resonant Frequency Hz.	Magness Taylor Firmness N.	Predicted ¹ ME MPa.
181.1	980	76.8	4.516
224.3	895	78.9	4.341
184.5	992	77.5	4.678
309.9	858	78.1	4.944
161.1	1013	85.3	4.463
216.0	952	76.4	4.794
195.5	964	75.6	4.592
208.3	984	77.5	4.995
169.6	1070	80.0	5.143
181.7	1000	78.0	4.702
167.3	1025	82.4	4.682
179.2	1013	80.2	4.789
207.5	939	68.7	4.534
178.9	1029	75.4	4.924
230.0	933	72.5	4.802
178.8	1000	78.6	4.650
196.1	976	83.2	4.723
164.4	1109	82.4	5.418
154.3	1066	76.8	4.798
171.2	1000	77.0	4.527
284.6	838	70.9	4.458
165.7	1000	84.6	4.421
259.8	891	78.6	4.740
195.9	1009	82.4	5.027
203.6	1000	76.2	5.076
295.4	874	77.3	4.974
182.3	976	77.5	4.496
277.6	840	64.9	4.406
184.7	1010	77.0	4.853
182.8	988	79.2	4.607
177.2	1004	75.1	4.670
138.4	1094	86.5	4.697
252.3	882	69.7	4.564
179.7	1000	83.7	4.667
198.8	964	74.9	4.639
165.9	1000	77.5	4.421
210.4	927	76.8	4.461
231.5	948	86.2	4.968
204.6	980	78.9	4.891
229.1	915	77.6	4.605
188.2	1019	82.9	5.007
178.3	1021	80.5	4.847
164.4	1090	84.6	5.234
201.5	952	73.5	4.570
169.6	1021	85.0	4.683
221.7	891	80.5	4.264
214.4	900	72.7	4.259
186.5	972	79.2	4.524

Table A1. continued.

203.3	976	85.4	4.835
185.8	939	79.2	4.207
175.2	984	68.9	4.452
258.9	878	72.1	4.591
217.0	903	78.6	4.327
185.9	1000	78.4	4.771
214.8	958	77.8	4.825
216.3	915	74.9	4.429
165.0	1013	83.4	4.536
174.5	1045	75.6	5.002
163.4	1037	82.7	4.715
194.3	939	79.1	4.342
231.6	909	74.6	4.571
194.7	891	65.9	3.910
233.3	854	66.4	4.058
199.1	939	83.5	4.416
229.0	903	79.5	4.485
192.7	927	80.0	4.203
213.8	915	72.3	4.388
191.2	970	73.9	4.586
173.6	897	81.5	3.671
208.3	939	63.4	4.549
216.4	878	79.8	4.078
266.9	842	76.2	4.309
214.4	842	72.8	3.727
196.1	915	81.8	4.151
184.8	952	77.2	4.308
297.4	793	66.4	4.113
192.9	970	75.2	4.602
226.2	866	73.0	4.089
211.6	884	69.0	4.070
203.4	903	80.5	4.139
135.9	1025	65.3	4.150
204.8	927	78.1	4.450
197.0	903	65.8	4.077
173.1	952	68.7	4.236
223.2	891	86.9	4.295
248.6	903	63.8	4.785
252.8	891	62.8	4.708
183.7	915	68.7	4.039
210.6	878	66.8	4.025
186.7	921	65.3	4.112
238.	866	64.3	4.241
263.7	830	59.9	4.159
216.8	775	67.8	3.221
202.4	921	67.3	4.373
224.5	934	67.3	4.783
224.2	933	67.8	4.766
261.4	891	71.2	4.834
164.9	921	72.7	3.778
185.0	952	71.2	4.366
270.3	879	59.9	4.757

Table A1. continued.

243.2	793	57.0	3.630
205.1	903	73.7	4.190
192.6	921	62.4	4.206
203.3	884	58.4	3.986
169.6	939	57.9	3.979
207.2	866	57.4	3.863
176.3	903	62.4	3.780
229.9	866	60.9	4.145
187.0	915	53.0	4.045
184.4	909	58.4	4.005
191.3	878	64.8	3.803
188.2	921	68.2	4.089
228.3	842	57.0	3.920
207.6	921	64.8	4.365
185.5	952	71.7	4.376
251.9	854	62.4	4.289
210.8	939	58.4	4.647
206.7	842	60.4	3.623

1. Predicted modulus of elasticity by the model. The model uses measured density, mass, the uncut resonant frequency and a Poisson's ratio of 0.3.

Table A2. Data obtained from CA Law Rome apples.

Apple Mass	Peak Resonant Frequency	Measured ME	Predicted ¹ ME
239.4	878	4.506	4.365
229.6	988	4.867	5.372
231.7	927	4.588	4.755
219.3	927	4.507	4.597
235.9	915	4.873	4.689
175.5	982	5.008	4.438
221.4	939	4.872	4.743
234.5	903	4.482	4.551
180.2	1025	4.167	4.924
224.6	1025	4.581	5.696
231.8	939	3.888	4.887
206.0	988	3.925	5.000
245.5	982	4.131	5.559
227.8	939	3.998	4.822
224.7	939	3.840	4.787
232.4	933	4.013	4.835
210.1	969	3.998	4.877
265.7	878	3.611	4.675
249.4	848	3.634	4.183
192.3	976	4.012	4.661
177.6	988	4.349	4.527
219.8	933	4.325	4.659
214.9	921	3.937	4.468
213.5	939	4.894	4.620
255.0	860	4.642	4.373
204.4	958	4.821	4.676
212.3	878	4.424	4.033
219.0	915	4.616	4.471
194.6	927	5.124	4.238
231.7	933	4.834	4.826
221.0	891	4.313	4.261
189.3	1025	4.616	5.085
200.5	976	4.192	4.794
200.1	903	4.725	4.103
234.6	939	4.373	4.923
198.2	964	4.155	4.646
209.9	891	4.482	4.110
242.1	849	4.288	4.113
229.7	878	4.243	4.244
242.5	842	4.131	4.056
220.8	927	3.292	4.601
182.7	878	3.549	3.648
252.4	878	2.919	4.529
217.1	902	3.378	4.324
210.8	915	3.452	4.355
224.2	878	3.294	4.188
183.0	976	3.978	4.516
206.4	903	3.333	4.184
209.5	958	4.314	4.758

Table A2. continued.

255.9	836	3.293	4.133
-------	-----	-------	-------

1. Predicted modulus of elasticity by the model. The model uses measured density, mass, the uncut resonant frequency and a Poisson's ratio of 0.3.

Table A3. Data obtained from Paula Red apples.

Apple Mass kg.	Density kg/m ³	Freq. (uncut) Hz.	Freq. (cut) Hz.	ME ¹ MPa.	ME ² MPa.	ME ³ MPa.	ME ⁴ MPa.
207.9	754	805	781	3.794	3.276	3.083	3.105
195.6	804	866	817	3.932	3.718	3.309	3.263
193.6	779	854	830	4.262	3.554	3.357	3.345
228.3	768	805	781	3.795	3.509	3.302	3.305
200.5	780	842	817	3.730	3.538	3.331	3.317
222.8	747	793	769	3.502	3.318	3.120	3.153
195.3	786	842	817	3.995	3.482	3.278	3.256
202.1	762	842	805	3.416	3.528	3.225	3.237
200.2	765	866	830	3.561	3.715	3.413	3.420
199.6	785	878	854	3.942	3.844	3.636	3.614
192.4	780	939	903	4.236	4.281	3.959	3.942
213.9	771	915	830	4.023	4.346	3.576	3.575
204.8	773	903	878	3.722	4.115	3.891	3.886
197.7	767	854	830	4.416	3.586	3.387	3.392
212.5	780	891	817	3.695	4.119	3.463	3.448
224.7	786	830	805	3.612	3.719	3.499	3.475
197.6	773	866	842	3.709	3.696	3.494	3.489
196.7	764	866	830	3.589	3.670	3.371	3.380
201.9	770	805	781	3.071	3.235	3.045	3.045
205.1	771	915	830	4.042	4.226	3.477	3.476
209.6	797	817	793	3.594	3.456	3.256	3.219
202.7	791	842	817	3.715	3.581	3.371	3.341
213.1	781	793	769	3.767	3.270	3.075	3.061
198.1	772	854	817	3.469	3.599	3.294	3.291
221.5	774	805	781	3.673	3.447	3.245	3.239
203.5	774	878	866	3.990	3.870	3.765	3.758
191.1	759	842	805	3.565	3.395	3.104	3.119
200.4	743	878	854	4.059	3.785	3.581	3.623
218.5	745	854	817	3.886	3.797	3.475	3.513
197.3	769	854	830	3.849	3.585	3.386	3.387
207.8	769	817	781	3.634	3.396	3.103	3.104
197.1	775	817	781	3.553	3.286	3.003	2.997
199.2	754	830	793	3.512	3.382	3.087	3.110
216.7	752	817	781	3.862	3.466	3.167	3.192
213.2	770	805	781	3.618	3.353	3.156	3.156
202.9	762	781	744	3.295	3.046	2.764	2.773
205.5	795	793	769	3.618	3.211	3.020	2.988
209.4	766	793	769	3.219	3.211	3.020	3.025
219.2	785	781	756	3.429	3.238	3.034	3.014
202.1	779	781	756	3.050	3.059	2.866	2.855
192.4	752	781	744	3.287	2.925	2.655	2.676
199.9	760	756	720	2.979	2.822	2.560	2.571
211.7	787	744	708	3.136	2.873	2.602	2.583
193.2	789	744	708	2.932	2.705	2.450	2.430
214.4	777	756	720	3.218	2.979	2.702	2.694
198.7	673	732	695	2.834	2.525	2.277	2.381
201.2	764	793	769	3.387	3.123	2.936	2.944
202.5	779	744	708	2.584	2.780	2.517	2.508

Table A3. continued.

206.8	749	732	683	3.070	2.694	2.345	2.367
214.3	799	756	732	3.038	3.003	2.815	2.781
207.1	753	756	720	2.464	2.880	2.612	2.632
205.4	788	756	720	2.860	2.909	2.639	2.618
211.3	741	756	720	2.665	2.905	2.635	2.668
196.5	759	805	769	3.130	3.162	2.886	2.900
195.8	771	756	720	2.715	2.797	2.537	2.536
206.6	779	720	695	2.689	2.638	2.458	2.449
192.2	749	720	695	2.202	2.481	2.312	2.334
216.2	763	756	720	2.886	2.978	2.701	2.709
207.9	757	756	720	2.428	2.893	2.624	2.639
213.4	730	744	708	2.661	2.818	2.551	2.597
217.2	827	720	695	2.471	2.783	2.593	2.532
205.6	783	708	671	2.617	2.547	2.288	2.275
216.9	754	695	646	2.493	2.512	2.170	2.186
195.1	771	769	732	2.830	2.887	2.616	2.614
200.4	717	683	646	2.214	2.263	2.025	2.073
211.6	791	708	683	2.416	2.605	2.424	2.403
194.4	683	720	683	2.501	2.425	2.182	2.271
194.8	772	756	720	2.803	2.789	2.530	2.527
212.2	822	756	732	2.499	3.015	2.827	2.766
205.8	719	708	683	2.450	2.478	2.306	2.359

1. Measured modulus of elasticity.

2. Predicted modulus of elasticity by the model. The model uses measured density, mass, the uncut resonant frequency and a Poisson's ratio of 0.3.

3. Predicted modulus of elasticity by the model. The model uses measured density, mass, the cut resonant frequency and a Poisson's ratio of 0.3.

4. Predicted modulus of elasticity by the model. The model uses an assumed constant density of 770 kg/m^3 , mass, the uncut resonant frequency and a Poisson's ratio of 0.3.

Table A4. Data obtained from Golden Delicious apples.

Apple Mass kg.	Density kg/m ³	Freq. (uncut) Hz.	Freq. (cut) Hz.	ME ¹ MPa.	ME ² MPa.	ME ³ MPa.	ME ⁴ MPa.
177.2	894	1135	1098	4.987	6.192	5.794	5.513
174.3	813	1025	1001	4.363	4.837	4.613	4.530
245.8	793	939	915	4.456	5.058	4.802	4.755
218.5	799	1025	1001	4.851	5.588	5.329	5.265
217.3	781	939	903	4.248	4.640	4.291	4.271
222.1	782	927	903	3.823	4.594	4.358	4.337
175.0	803	1062	1013	4.669	5.191	4.722	4.657
234.9	785	927	915	4.286	4.765	4.642	4.612
174.8	806	1098	1062	4.436	5.534	5.176	5.099
176.2	807	1147	1098	4.914	6.089	5.580	5.492
214.6	833	1013	988	4.327	5.467	5.200	5.066
222.8	799	939	903	4.885	4.747	4.390	4.337
225.6	781	952	927	4.713	4.887	4.634	4.611
223.0	811	976	927	4.676	5.170	4.664	4.584
214.1	790	976	939	4.655	4.986	4.615	4.576
174.4	809	1086	1074	4.697	5.422	5.302	5.215
176.2	822	1049	1013	4.567	5.125	4.779	4.675
174.5	817	1062	1025	4.954	5.201	4.845	4.750
175.7	803	1037	1001	4.534	4.949	4.611	4.548
174.6	817	1098	1049	4.767	5.560	5.074	4.975
180.2	799	1025	952	3.567	4.919	4.243	4.191
223.1	820	988	952	4.357	5.318	4.937	4.835
250.2	819	878	854	4.128	4.530	4.286	4.198
270.9	789	830	805	3.658	4.209	3.959	3.927
225.4	802	952	927	4.262	4.930	4.674	4.611
175.2	801	1049	1013	3.761	5.061	4.719	4.657
172.6	796	1049	1001	4.239	4.992	4.545	4.495
174.8	812	1110	1062	3.936	5.671	5.190	5.099
154.5	809	1062	1025	4.121	4.779	4.451	4.379
172.4	804	1049	1013	4.119	5.009	4.671	4.604
180.8	804	988	976	3.363	4.579	4.468	4.405
239.7	810	866	842	3.685	4.262	4.028	3.961
236.9	797	842	830	3.691	3.974	3.861	3.816
244.0	822	891	866	4.296	4.595	4.341	4.248
225.2	806	939	927	4.051	4.805	4.683	4.611
172.4	796	964	939	3.554	4.217	4.000	3.956
158.6	798	976	964	3.437	4.087	3.987	3.940
158.8	810	1025	1013	3.772	4.531	4.425	4.351
177.8	805	879	854	3.145	3.586	3.384	3.335
176.6	807	939	915	3.793	4.081	3.875	3.814
222.3	802	830	817	3.289	3.714	3.598	3.550
238.2	789	878	866	3.837	4.330	4.212	4.178
238.4	805	854	830	3.376	4.124	3.895	3.838
241.6	811	817	775	3.395	3.816	3.433	3.374
175.1	801	921	903	3.567	3.901	3.750	3.701
153.9	813	1062	1025	3.806	4.766	4.439	4.360
226.8	809	854	839	3.562	3.991	3.851	3.789
172.5	804	1001	976	3.685	4.561	4.336	4.274

Table A4. continued.

153.0	817	1025	1013	3.576	4.447	4.343	4.258
173.3	800	1013	1001	4.253	4.681	4.571	4.513
181.4	802	878	854	2.542	3.627	3.431	3.385
194.2	789	866	854	2.732	3.676	3.574	3.545
178.7	805	775	756	2.674	2.798	2.663	2.623
154.8	811	878	854	3.191	3.269	3.093	3.040
231.2	801	756	744	2.248	3.163	3.063	3.023
219.0	813	775	756	2.684	3.224	3.067	3.012
192.0	809	815	775	2.901	3.260	2.948	2.900
227.4	804	775	744	2.148	3.290	3.031	2.988
223.7	817	756	732	2.861	3.110	2.915	2.858
189.3	800	854	830	3.127	3.529	3.333	3.291

1. Measured modulus of elasticity.

2. Predicted modulus of elasticity by the model. The model uses measured density, mass, the uncut resonant frequency and a Poisson's ratio of 0.3.

3. Predicted modulus of elasticity by the model. The model uses measured density, mass, the cut resonant frequency and a Poisson's ratio of 0.3.

4 Predicted modulus of elasticity by the model. The model uses an assumed constant density of 812 kg/m^3 , mass, the uncut resonant frequency and a Poisson's ratio of 0.3.

BIBLIOGRAPHY

- Abbott, J.A., G.S. Bachman, N.F. Childers, J.V. Fitzgerald
1968 and F.J. Matusik,
Sonic techniques for measuring texture of fruits
and vegetables. Food Technology. 22(5):101-112
- Abbott, J.A., G.S. Bachman, N.F. Childers, J.V. Fitzgerald
1968 and F.J. Matusik,
Acoustic vibration for detecting textural quality
of apples. American Society of Hort. Sc., 93:725
- Auchenbach, J.D.
1973 Wave Propagation In Elastic Solids. American
Elsevier Publishing Company, Inc., New York
- Auld, B.A.
1973 Acoustic Fields and Waves In Solids. (Vol. I &II),
John Wiley and Sons, New York
- Bitner, D. R. and K.H. Norris
1968 Optical properties of selected fruits versus
maturity. Transactions of the ASAE, 11(4):536-543
- Clark, R.L. and P.S. Shackelford, Jr.
1973 Resonance and optical properties of peaches as
related to flesh firmness. Transactions of the
ASAE, 16(6):1140-1142
- Clark and Mickelson
1942 Fruit firmness tester. US patent #2,277037
- Cook, J.R.
1972 An interpretation of the resonant behavior of
intact fruits and vegetables. Transactions of the
ASAE, 1075-1080
- Cook, J. R. and R.H. Rand
1973 A mathematical study of resonance in intact fruits
and vegetables using a 3-media sphere. JAER, 18,
141-157
- Cook, J.R.
1970 A theoretical analysis of the resonance of intact
apples. Paper # 70-345, ASAE, St. Joseph, MI. 49085
- De Baerdemaeker, J., L. Lemaitre and R.Meire
1982 Quality detection by frequency spectrum analysis
of the fruit impact force. Transactions of the
ASAE, 175-178

- Delwiche, M. J. and S. V. Bowers
1986 Theory of fruit firmness sorting by impact forces.
Paper # 86-3027, ASAE, St. Joseph, MI. 49085
- Delwiche, M. J. and S. V. Bowers
1985 Signal processing of fruit impact forces for
firmness detection. Paper # 85-3029, ASAE,
St. Joseph, MI. 49085
- Eringen, A.C.
1975 Elastodynamics. Academic Press, New York
- Finney, E.E. and K.H. Norris
1968 Instrumentation for investigating dynamic
mechanical properties of fruits and vegetables.
Transactions of the ASAE, 11(2):94-97
- Finney E.E.
1971 Dynamic elastic properties and sensory quality of
apple fruit. Journal of Texture Studies 2:62-74
- Finney E.E., I. Ben-Gera and D.R. Massie
1968 An objective evaluation of changes in firmness of
ripening bananas using a sonic technique. Journal
of Food Science. 32(6):642-646
- Finney E.E.
1970 Mechanical resonance within red delicious apples
and its relation to fruit texture. Transactions of
the ASAE, 13(2):177-180
- Finney E.E.
1971 Random vibration techniques for non-destructive
evaluation of peach firmness. JAER, 16(1):81-87
- Finney, E.E.
1969 Objective measurements for texture in foods.
Journal of Texture Studies, 1, 19
- Fridley R.B., P. Chen, J. J. Mehlchau and L.L. Claypool
1974 Mechanical sensing of pear maturity for improved
cold storage. Paper # 74-3041, ASAE, St. Joseph,
MI. 49085
- Garret, R.E. and R.B. Furry
1972 Velocity of sonic pulses in apples. Transactions
of the ASAE, 15(4):770-774
- Hood, C.E., B.K. Webb, R.A. Baumgardner, T.R. Garret,
1976 B.L. Hair, and C.E. Gambrell.
Maturity sorting of peaches with the FMC color
sorter. Paper # 76-3031, ASAE, St. Joseph MI.
49085

Lamb, H

- 1882 On the vibrations of an elastic sphere.
Proceedings of the London Mathematical Society,
Vol xiii, 51-66.

Lott, R.V.

- 1965 The relationship between stage of maturation and
degree of quality in apple and peach fruits.
Transactions of the Illinois Horticultural
Society. 99,139

Love, A.H.

- 1944 A Treatise on the Mathematical Theory of
Elasticity. Dover Publications, New York.

Mizrach, A., N. Galili and G. Rosenhouse

- 1988 Determination of fruit and vegetable properties by
ultrasonic excitation. Paper # 88-6019, ASAE,
St. Joseph MI.
49085

Mohsenin N.N.

- 1980 Physical Properties of Plant and Animal Materials.
Gordon And Breach Science Publishers, New York

Nahir D., Z. Schmiloovitch and B. Ronen

- 1986 Tomato grading by impact force response. Paper #
86-3028, ASAE, St. Joseph MI. 49085

Nybohm N.

- 1962 A new principle for measuring firmness of fruits.
Horticultural Research 2(1)

Sato, Y. and T. Usami

- 1962 Basic study on the oscillations of a homogeneous
elastic sphere I, frequency of oscillations.
Geophysics Magazine 31,15

Sato, Y. and T. Usami

- 1962 Basic study on the oscillations of a homogeneous
elastic sphere II, distribution of displacement.
Geophysics Magazine 31,25

Sato, Y. and T. Usami

- 1962 Basic study on the oscillations of a homogeneous
elastic sphere III, boundary conditions and the
generation of elastic waves. Geophysics Magazine
31,49

Shpolyanskaya A.L.

- 1952 Structural mechanical properties of wheat grain.
Colloid Journal(USSR), 14(1):137-148 Translated by
Consultant Bureau, New York

Seymour, S.K. and D.D. Hamman

- 1984 Design of a microcomputer based instrument for crispness evaluation of food products.
Transactions of the ASAE, 27(4):1245-1250

Z USDA

- 1978 APPLES, Shipping Point Inspection Instructions,
United States Department of Agriculture
Agricultural Marketing Service, Fruit and
Vegetable Division, Fresh Products Branch,
Washington, D.C.

Yamamoto, H., M. Iwamoto and S. Haginuma

- 1980 Acoustic impulse response method for measuring
natural frequency of intact fruits and preliminary
applications to internal quality evaluations of
apples and watermelons. Journal of Texture
Studies 11:117-136

MICHIGAN STATE UNIV. LIBRARIES



31293005923713